DOI: 10.1039/D0EN00486C

Nanobiochar: Production, Properties, and Multifunctional Applications

Sammani Ramanayaka[1], Meththika Vithanage[1,*], Daniel S. Alessi[2], Wu-Jun Liu[3], Anil C.A. Jayasundera[4], Yong Sik Ok[5,*]

[1]Ecosphere Resilience Research Center, Faculty of Applied Sciences, University of Sri Jayewardenepura, Nugegoda, Sri Lanka

[2]Department of Earth and Atmospheric Sciences, University of Alberta, Edmonton, Alberta T6G 2E3, Canada

[3]CAS Key Laboratory of Urban Pollutant Conversion, Department of Applied Chemistry, University of Science & Technology of China, Hefei, 230026, China

[4]Department of Chemistry, University of Peradeniya, Peradeniya, Sri Lanka

[5]Korea Biochar Research Center, APRU Sustainable Waste Management & Division of Environmental Science and Ecological Engineering, Korea University, Seoul 02841, South Korea

Corresponding Authors:

meththika@sjp.ac.lk

yongsikok@kore.ac.kr

Author emails:

sammani@sci.sjp.ac.lk

alessi@ualberta.ca

liuwujun@mail.ustc.edu.cn

acaj@pdn.ac.lk

Abstract

Nanobiochar has received much recent attention among engineered biochars owing to its useful chemical and physical properties. Research efforts have attempted to discover novel methods for nanobiochar preparation and applications. In this review, we summarize all the reported literature on various aspects of nanobiochar preparation, production and use. Often, bulk parent biochar obtained from biomass pyrolysis, mechanically ground using different milling processes to fabricate nanobiochar. Apart from mechanical means, direct fabrication of nanobiochar through flash heating resulting in graphitic nanosheets have been reported. Process conditions applied to the parent biochar directly influence the properties of the resulting nanobiochar. For instance, over 70% out of 33 nanobiochars derived from biomass pyrolyzed above 450 °C demonstrated 32 times greater BET specific surface areas than nanobiochars produced at <450 °C. Nanobiochar has diverse applications, such as wastewater treatment, health care applications, use as an electrode material, and in supercapacitors and sensors, owing to its wide range of physical and chemical properties. However, the toxicity of nanobiochar to human and ecosystem health has not received sufficient research attention. More research should be performed to elucidate the drawbacks, such as high agglomeration potential and low yield, of nanobiochar for practical uses. Furthermore, reported data is insufficient to obtain a clear idea of the nature and behavior of nanobiochar, despite growing interest in the research topic. Hence, future research should be driven towards exploring techniques to improve the yield of nanobiochar, reduce agglomeration, upscale it for electrode supercapacitor production and understanding toxicological aspects.

Key words: Clean water and sanitation, Green and sustainable remediation, charcoal, nanotechnology, black carbon, soil remediation

Introduction

The concept of biochar dates back to the ancient Amerindian civilizations in the South American Amazon region [1]. Studies on the Amazonian dark earth, a human-made soil mixture also known as *terra preta*, reveal that a carbonaceous material similar to biochar was used by these ancient civilizations [2,3] to improve soil fertility and crop productivity. Similar carbon-rich materials have been used by humankind for centuries; however, the term "biochar" was introduced by scientists to describe a pyrogenic carbonaceous solid material prepared in oxygen-free environments at high temperatures, which was known as "agrichar" at the time [4]. Hydrochar is a similar form of charred organic matter, however different from biochar in terms of carbon stability and production methods [5]. Pyrolysis, dry carbonization, and gasification of waste biomass, such as agricultural waste, forest residues, municipal solid waste, and animal manure, results in biochar [6,7]. Depending on the feedstock material, technique of production, pyrolysis temperature, and other pre- or post-processing factors, biochar can have a range of properties, leading to a wide variety of applications garnering high interest among researchers [8]. For instance, pyrolysis of biomass under oxygen free environments between 300-700 °C as well as gasification of biomass at high temperatures (from 800 to 1000 °C) results biochar, while torrefaction at temperatures from 200-300 °C produces bio-coal having different characteristics [9–11].

Biochar is commonly used, among its various environmental applications, as an option for solid waste management, and as a material for soil amendment, water treatment, and carbon sequestration [3]. Furthermore, biochar is now being explored for energy production, healthcare applications, and for use in electrodes, supercapacitors, and sensors, owing to its unique and diverse properties [12–15]. These properties, including adsorptive removal capability, can be enhanced by various pre- and post-activation techniques. The high porosity, functional groups and surface area of biochar strongly assist in the immobilization of various contaminants, including potentially toxic elements and persistent organic compounds [16]. A large number of functional groups on the biochar surface support the adsorption of organic and inorganic contaminants in aqueous media [17].

In this review, we consider biochars having particle sizes of 1 μm or greater as macrobiochar, 1 μm – 100 nm as colloidal biochar, and <100 nm as nanobiochar, respectively [18]. Beyond macrobiochar, engineered biochars have gained recent research attention, owing to its enhanced properties. Nanobiochar has a markedly higher surface area to mass ratio than macrobiochar, and apart from that, there are multiple potential applications of nanobiochar

other than as an adsorbent; for example, as a sensor, capacitor and photocatalytic material. Scaling down biochar to the nanoscale, using top-down approach, is the most common method to prepare nanobiochar. The physicochemical and mechanical properties of nanobiochar are crucial indicators in determining its applications. Certain properties, such as biochar yield, elemental composition, surface area, and porosity, are governed by feedstock characteristics, the production process, temperature, and residence time [19]. However, biochar properties can be improved using pre- and post-modification techniques [20]. The relative fractions of lignin, cellulose, and hemicellulose in lignocelluosic biomass play a major role in the dominant properties of the final biochar product [21]. A general trend of increasing hydrophobicity and aromaticity with decreasing product yield and surface functional groups is observed with an increased degree of carbonization [19]. The surface area and the breakdown of the fibrous biomass structure are also affected by the degree of carbonization. Meanwhile, the density and mechanical stability are strongly influenced by pores produced by the devolatilization of gases; however, these properties have not received much attention from researchers [22]. Brittleness, on the other hand, is added to biochar during carbonization, and mechanical stability improves the grindability of the material [23]. Mechanical grinding leads to a new approach to the manufacture of biochar, where the material can be engineered by the reduction of particle size to the nanoscale. This topic has recently become a new focus of research.

Mechanical grinding is the most common technique used in the production of nanobiochar [24]. The top-down approach, a method of breaking down the macrostructure to the nanoscale, is commonly followed in the method of preparation [25]. Nanobiochar is unique from its pristine form, owing to the strikingly greater surface area, graphitic nature, highly negative zeta-potential and wide variation of crystalline forms [29]. Furthermore, nanobiochar demonstrates a better stability and temperature-dependent dispersibility than the bulk biochar [18]. Similarly, nanobiochars are rich in humic-like fluorescent components and reactive organic substances, properties which give them potential to be applicable in high-tech applications such as batteries, supercapacitors and sensing technologies. In the first attempt of nanobiochar preparation, sawdust was successfully modified to form a solid acid catalyst using a fast pyrolysis–sulfonation process [26]. Saxena et al. (2014) demonstrated an enhanced growth rate of wheat by the application of hydrophilic carbon nanoparticles from rice plant waste biochar [27]. It is interesting to note that the high temperature thermal-chemical flash exfoliation produces carbon nanosheets with high specific surface area [28]. In 2016, Oleszuczuk and colleagues reported the first publication on nanobiochar characterization. They produced various

nanobiochars which, upon characterization, showed considerable structural and chemical differences to their macroscopic counterparts [29]. Only few publications appeared on the topic of nanobiochars from 2013 until 2017, however, thereafter, the number of publications per year increased (Figure 1). Given the growing recent interest, the objective of this review is to summarize the results of the studies on nanobiochar that have reported thus far in order to provide a critical analysis of knowledge gaps and thereby explore insights for future research in a holistic way.

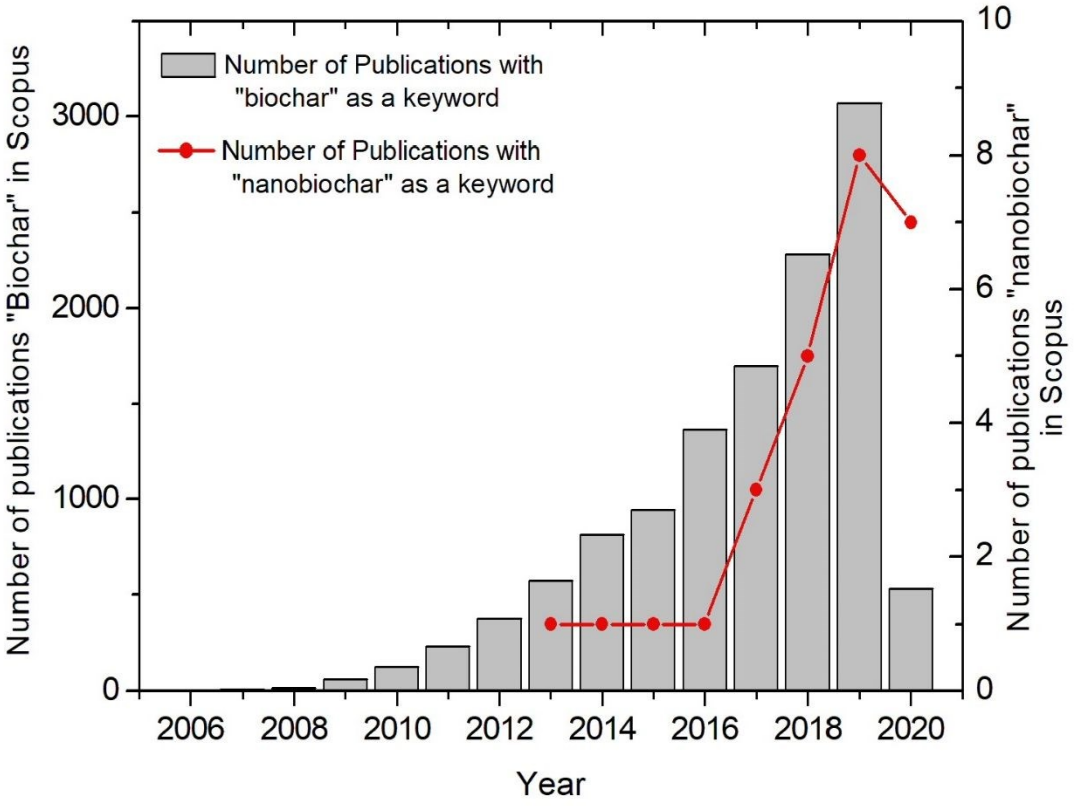

Figure 1. Number of publications on “biochar” and “nanobiochar” as keyword search based on the data in the Scopus database from 2006 – 2020 (By 29th February, 2020)

2.0 Nanobiochar Production

Nanobiochar is an emerging type of advanced nanostructured material. The majority of production and research on nanobiochar is currently conducted by green synthesis methods and using energy-saving strategies in nanotechnology. Studies to date indicate that nanobiochar is characterized by significant physical and chemical differences, such as higher surface areas,

View Article Online
DOI: 10.1039/D0EN00486C

larger pore volumes, smaller hydrodynamic radius, stronger negative zeta potentials, more oxygen–containing functional groups, and carbon defects which may generate reactive organic species (ROS), thereby increasing adsorption capacities as compared to its macrochar counterparts, and having properties more similar to black carbon [29–31].

2.1 Feedstock materials

Agricultural waste, wood and forest residues, municipal solid waste, animal manure, and sewage sludge are commonly used as feedstock materials in the preparation of biochar [29]. On the other hand, agricultural waste, wood, and forest residues have been applied as feedstock for nanobiochar, with commonly used feedstock materials including sugar cane bagasse, rice husk, peanut shell, rice straw, bamboo, grass, oil palm empty fruit bunch, soy bean stover and wood (Table 1). Feedstock material directly influences the resulting type of nanobiochar, as in the case of macrobiochars. Among reported nanobiochar types, more than 98% are engineered nanobiochars were manufactured via mechanical grinding. Genovese et al. (2015) and Li et al. (2017) investigated the use of a natural layered nanosheets from corn cob and soy bean stover, which are low-cost agricultural waste[11,29]. In this particular novel nanobiochar synthesis method, biomass pre-treatment was followed by thermal-chemical flash exfoliation to obtain nanosheets without resorting to grinding [28,32,33,28]. New methods for nanobiochar production, such as microwave pyrolysis, have also been reported in the literature. Furthermore, softwood biomasses (e.g., softwood chips and hemp stalk) have successfully utilized in the preparation of nanobiochar [34].

Table 1. Different types of nanobiochar, their feedstock materials, and applications/focus with varying temperatures/microwave power levels

Nanobiochar type	Feedstock material	Application/focus	Temperature/ Power °C/W	Reference
Baggase biochar (BGBC)	Sugarcane baggase	Metal ion removal [Ni(II)]	300 °C	35
			450 °C	
			600 °C	
	Baggase	Magnetic biochar nanoparticles for bisphenol A sensing in water	900 °C	36
Ball-milled baggase biochar*		As an alternative carbon electrode	300 °C	37
			450 °C	
			600 °C	
		For enhanced sorption of CO_2 and reactive red	450 °C	38
			600 °C	
		Removal of sulfamethoxazole and sulfapyridine antibiotics from aqueous environments	300 °C	39
			450 °C	
			600 °C	
		Removal of aqueous methylene blue	300 °C	30
			450 °C	
			600 °C	
Bamboo biochar (BBBC)	Bamboo	Metal ion removal [Ni(II)]	300 °C	35
			450 °C	

			600 °C	
Ball-milled bamboo biochar*		Methylene blue removal	450 °C	[40]
		As an alternative carbon electrode	300 °C	[37]
			450 °C	
			600 °C	
		Removal of ammonium from water	450 °C	[41]
		Removal of sulfamethoxazole and sulfapyridine antibiotics from aqueous environments	300 °C	[39]
			450 °C	
			600 °C	
		Removal of aqueous methylene blue	300 °C	[30]
			450 °C	
			600 °C	
Ball-milled hickory wood biochar*	Hickory wood	Removal of volatile organic compounds	300 °C	[42]
			450 °C	
			600 °C	
		For enhanced sorption of CO_2 and reactive red	450 °C	[38]
		Removal of sulfamethoxazole and sulfapyridine antibiotics from aqueous environments	300 °C	[39]
			450 °C	
			600 °C	
		Removal of aqueous methylene blue	300 °C	[30]

			450 °C	
			600 °C	
Wood biochar	Hickory wood	Metal ion removal [Ni(II)]	300 °C	35
			450 °C	
			600 °C	
	Pinewood	Chitosan-nanobiochar composite as nanobiocatalyst	525 °C	43
		Carrier for the immobilization of crude laccase by covalent bonding	525 °C	44
		Contaminant removal (carbamazepine)	525 °C	45
		A green method for production of nanobiochar by ball-milling	525 °C	24
	Wood chip	Effects of ball-milling on the photochemistry of biochar	300 °C	46
			500 °C	
			700 °C	
		Characterization of physicochemical properties	500 °C	47
	Pitch pine	Nano-powders of biochar as an electrode material for voltametric sensor [Pb(II) and Cd(II)]	600 °C	48

	Dendro wood	Removal of organic and inorganic contaminants [oxytetracycline, glyphosate, Cd(II), and (Cr(VI)]	700–1000 °C	49
	Ball-milled poplar wood*	Toxicity induction in *Streptomyces*	500 °C	50
		Sorption of inorganic Hg^{2+} and organic CH_3Hg^+	300 °C	51
Iron oxide Permeated Mesoporous rice-husk nanobiochars (IPMN)	Rice husk	Metal ion removal [As(III)]	600 °C	4
Rice husk nanobiochar		Characterization of physicochemical properties	500 °C	47
		Adsorption of phthalate esters	500 °C	52
Ball-milled rice husk biochar*		Adsorption of galaxolide	300 °C	53
			500 °C	
			700 °C	
		Production of a bio-filler for reinforcement of rubber mechanical property	-	54
Goethite modified peanut shell biochar (PSB)	Peanut shell	Characterization of physicochemical properties	300 °C	18
			400 °C	
			500 °C	
			600 °C	

			700 °C	
Peanut shell nanobiochar		Characterization of physicochemical properties	500 °C	47
Magnetic nanobiochar (MBC)	Oil palm empty fruit bunches	Preparation of magnetic solid acid catalyst	500 °C	55
			600 °C	
Sulfonated biochar			500 °C	
			600 °C	
Grass biochar	Elephant grass (BC-m) (*Miscanthus*)	Characterization of nanoparticles of biochars from different biomass	700 °C	29
	Wicker (BC-w)	Characterization of nanoparticles of biochars from different biomass	700 °C	29
	Barley grass	Characterization of physicochemical properties	500 °C	47
Sorghum straw biochar	Sorghum straw	Biochar-derived carbonaceous nanomaterials for the detection of heavy metals in aqueous systems	500 °C	56
Wheat straw biochar	Wheat straw (BC-s)	Characterization of nanoparticles of biochars from different biomass	700 °C	29
		Characterization of physicochemical properties	500 °C	47
Wheat straw magnetic	Wheat straw	Tetracycline and Hg(II) ion removal	400 °C	57

biochar			550 °C 700 °C	
Ball-milled Wheat straw biochar*		Removal of galaxolide	300 °C 500 °C 700 °C	53
Exfoliated biochar nanosheets	Corn cob	Study high capacitive performance	900 °C	28
Corn straw nanobiochar	Corn straw	Adsorption of phthalate esters	500 °C	52
Ball-milled corn stover biochar*	Corn stover	Optimization of ball-milling parameters	-	58
Ball-milled Fe° -biochar composite*	Corn stalk	Removal of Cr(VI)	300 °C 500 °C 700 °C	59
Rice straw biochar	Rice straw	Goethite modified black carbon nanoparticle for phenanthrene removal	400 °C 700 °C	60
		Water soluble carbon nanoparticles to boost wheat (*Triticum aestivum*) plant growth	-	27
		Biochar-derived carbonaceous nanomaterials for the detection of heavy metals in aqueous systems	500 °C	56

Rice hull biochar	Rice hull	Agronomic benefits and potential risk of nanobiochar on rice plant growth and uptake of heavy metals	300 °C 600 °C	61
Fir sawdust biochar	Fir sawdust	Facile synthesis of highly efficient and recyclable magnetic solid acid from biomass waste	600 °C	26
Ball-milled sawdust biochar*	Sawdust	Effects of wet and dry ball-milling on the physicochemical properties	600 °C	62
Softwood biochar	Softwood chip (spruce–fir mix)	Synthesis and characterization of biochar	2100 W 2400 W 2700 W	34
	Hemp stalk		2100 W 2400 W 2700 W	
Animal manure	Dairy manure	Characterization of physicochemical properties	500 °C	47
		Biochar-derived carbonaceous nanomaterials for the detection of heavy metals in aqueous systems	700 °C	56

	Pig manure	Characterization of physicochemical properties	500 °C	47
Ball-milled bone biochar*	Cow bone meal	Removal of aquatic Cd(II), Cu(II) and Pb(II)	300 °C 450 °C 600 °C	63
Municipal source	Sewage sludge	Characterization of physicochemical properties	500 °C	47
Mixed biochar	Fresh wheat, rice straw, corn straw	Reduction of the allelopathic effect from *Imperata cylindrica* on rice seedlings	350 °C 650 °C	64
Black liquor lignin biochar	Hardwoods, wheat straw	Preparation of alternative for carbon black	800 °C	65
Ball-milled typha biochar*	*Typha angustifolia* plant	For the selective uptake of aquatic uranium	500 °C 700 °C	66
Ball-milled kenaf biochar*	Kenaf plant	Characterization of carbon particles	-	67

Note: * symbol represents ball-milled biochar which includes both nano and colloidal fraction

Agricultural waste contains a large amount of hemicellulose, while woody biomass contains more lignin. Better grindability has been reported for torrefied products from biomass with high hemicellulose content as compared to those with more lignin. Biomass torrefaction has been carried out in low oxygen environments at temperatures <300 °C, which results in bio-coal, whereas those produced at temperatures above 300 °C are considered to be biochar [68]. Literature reports that agricultural waste feedstock materials with high hemicellulose content result in good grindability and broad particle-size distributions [19].

2.2 Milling for nanobiochar fabrication

The synthesis of nanoparticles and fabrication of nanostructures can be achieved via two approaches: top-down and bottom-up [24]. The size of the bulk material is reduced to the nanoscale in the top-down approach, while the material is built up from the atomic scale in the bottom-up approach. Some of the technologies involved in the production of nanoparticles are costly. Therefore, a low-cost, green method is essential to counteract the high input energy, expensive precursors, and sophisticated processes that are otherwise required in nanoparticle fabrication methods [25]. Some researchers have used mechanical methods, such as cutting, etching, and grinding, to reduce the cost. Among these methods, ball-milling plays a major role in breaking the material down to nanoscale without damaging the crystal structure (Figure 2). The use of ball-milling for nanoparticle production has been studied widely in recent years, because of its low cost, large scale applicability, and low energy for production [69].

View Article Online
DOI: 10.1039/D0EN00486C

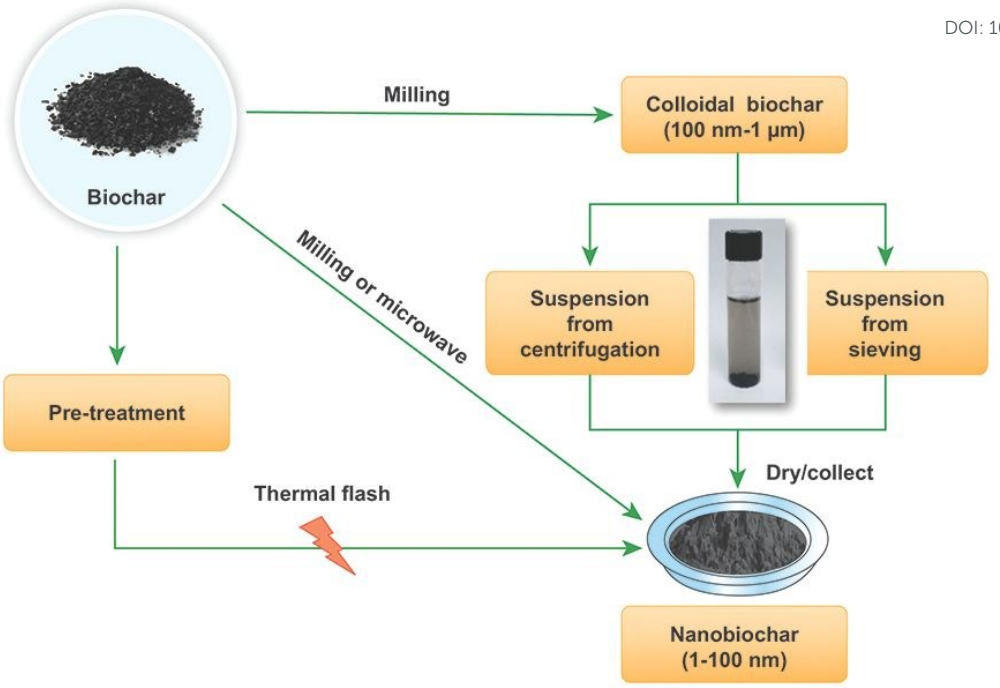

Figure 2. Preparation methodologies of pristine nanobiochar

Ball-milling is the method most favored by researchers for the production of nanobiochars. Both agate and stainless-steel balls have been used in the ball-milling process. The weight of balls used in milling depends on the ball diameter and the material. For pinewood and modified rice husk feedstock materials, 30–45 g of stainless-steel balls have been used, whereas sugar cane bagasse, bamboo, and hickory wood feedstocks have been milled with 180 g of agate balls (Table 2). Apart from the milling type, rotational speed, ball-to-power mass ratio, and milling time are among the parameters that can directly influence the resulting nanobiochar particle size and surface energy [70]. In a very recent study on the preparation of magnetic wheat straw nanobiochar, 100 g of agate balls were used in the ball-milling process for 12 h [57]. However, there are a lack of comprehensive studies that determine specific relationships between feedstock, temperature and other properties with changes in particle size.

Table 2. Various types of nanobiochars fabricated under different milling conditions, and their surface areas

Nanobiochar type	Feedstock material	Temperature/Power °C/W	BET surface area (m^2/g)	Milling Conditions						Reference
				Ball-mill type	Ball diameter and weight	Rotations per minute	Material and jar volume	Milling time	Biochar-to-balls mass ratio	
Baggase biochar (BGBC)	Ball-milled baggase	300 °C	10.8	Planetary ball-mill (PQ-N2, Across International)	6 mm / 180 g	300	Agate jar (500 ml)	12 h	1:100	30,35
		450 °C	331							
		600 °C	364							
		300 °C	10.8							37
		450 °C	331							
		600 °C	364							
		300 °C	10.8							39
		450 °C	331							
		600 °C	364							
Bamboo biochar (BBBC)	Ball-milled Bamboo	300 °C	8.3							30,35
		450 °C	299							
		600 °C	276							
		450 °C	298.6							71
		300 °C	8.3							37
		450 °C	299							

		600 °C	276							
		450 °C	-							41
		450 °C	304	Planetary ball-mill	6 mm / 180 g	300	Agate jar (500 ml)	12 h	-	38
		600 °C	401							
		300 °C	8.3							39
		450 °C	299							
		600 °C	276							
N-doped bamboo biochar	N-doped ball-milled bamboo	450 °C	441							38
		600 °C	473							
Wood biochar	Ball-milled hickory wood	450 °C	342							
		600 °C	430							
	N-doped ball-milled hickory wood	450 °C	497							
		600 °C	548							
	Ball-milled hickory	300 °C	5.6	Planetary ball-mill	-	300	-	12 h	1:100	42
		450 °C	284.7							
		600 °C	304.8							

	wood	300 °C	5.6	Planetary ball-mill (PQ-N_2, Across International)	6 mm / 180 g	300	Agate jar (500 ml)	12 h	1:100	[39]
		450 °C	309							
		600 °C	207							
		300 °C	5.6							[30,35]
		450 °C	309							
		600 °C	270							
	Pinewood	525 °C	47.3	PM-100 planetary ball-mill (Retsch Corporation, Germany)	2.4 mm / 45 g	575	Stainless steel jar (500 ml)	100 min	-	[24,43–45,72]
	Wood chip	300 °C	7.92	planetary ball-mill (F-P2000, China)	3 mm / 100 g	200	Agate jar (500 ml)	24 h	1:50	[46]
		500 °C	151							
		700 °C	156							
	Ball-milled poplar wood	500 °C	-	Focucy, F-P2000 planetary ball-mill	150 g	300	Agate jar	24 h	-	[50]

		300 °C	61.3	Ball-mill machine (F-P4000)	300 g	300	Agate jar (500 ml)	12 h	-	[51]
Iron oxide Permeated Mesoporous rice-husk nanobiochars (IPMN)	Rice husk	600 °C	1736.81	EGOMA Auriga Planetary Ball-mill (India)	5 mm / 30 g	500	Stainless steel (50 ml)	-	-	[4]
Rice husk Nanobiochar	Rice husk	500 °C	298	Planetary ball-mill	5 mm / 1 g	600	Agate jar (500 ml)	150 min	-	[52]
	Ball-milled rice husk	300 °C	9.3	Planetary ball-mill	5 mm	300	Agate jar (500 ml)	24 h	1:100	[53]
		500 °C	190							
		700 °C	329							
		-	179.2	XQM-2 planetary ball-mill	450 g	400	Zirconia jar (500 ml)	12 h	-	[54]
Magnetic nanobiochar (MBC)	Fe loaded oil palm empty fruit	500 °C	53.77	High-speed rotary mill	-	-	-	-	-	[55]
		600 °C	173.18							
Sulfonated		500 °C	38.51							

magnetic biochar	bunches	600 °C	67.61							
Wheat straw magnetic biochar	Wheat straw	400 °C	47.2	Planetary ball-mill	5 mm / 100 g	-	Agate jar (160 ml)	12 h	-	[57]
		550 °C	333.4							
		700 °C	296.3							
	Ball-milled wheat straw	300 °C	10.8	Planetary ball-mill	5 mm	300	Agate jar (500 ml)	24 h	1:100	[53]
		500 °C	289							
		700 °C	401							
Corn straw nanobiochar	Corn straw	500 °C	364	Planetary ball-mill	5 mm / 1 g	600	Agate jar (500 ml)	150 min	-	[52]
Corn stover biochar	Ball-milled corn stover	-	25-194	QM-3SP2 Planetary ball-mill	-	-	Stainless steel (500 ml)	6 h	-	[58]
Corn stalk biochar	Ball-milled corn stalk	300 °C	14	Planetary ball-mill	150 g	400	Stainless steel (500 ml)	48 h	-	[59]
		500 °C	80							
		700 °C	252							
Mixed biochar	Fresh wheat, rice straw, corn	350 °C	-	Planetary ball-mill	3-15 mm	350	Stainless steel	12 h	15:1	[64]
		650 °C	-							

	straw									
Black liquor lignin biochar	Hardwoods, wheat straw	800 °C	83.4	Planetary ball-mill	-	-	-	4 h	-	[65]
Saw dust biochar	Saw dust	600 °C	Dry ball-milled 360 Wet ball-milled 334	QM-3SP04-1 planetary ball-mill	6 and 10 mm	-	Stainless steel (100 ml)	12 h	-	[62]
Typha biochar	Ball-milled *Typha angustifolia*	500 °C 700 °C	433 405	planetary ball-mill	6 mm / 330 g	200	Agate jar (500 ml)	12 h	1:100	[66]
Kenaf biochar	Ball-milled kenaf biochar	-	-	High energy ball-mill 8000D Mixer/Mill	-	875	-	12 h	1:10	[67]
Bone biochar	Call-milled	300 °C 450 °C	35.5 200	Ball-milling machine	330 g	300	Agate jar	12 h	1:100	[63]

	cow meal	bone	600 °C	194

View Article Online
DOI: 10.1039/D0EN00486C

2.3 Other fabrication techniques

Despite the advantages of ball-milling in the production of nanosized particles, researchers have used conventional methods of grinding, followed by sieving the aqueous suspension to prepare nanobiochar (Table 3). Li et al. (2017), for example, prepared pitch pine nanobiochar by grinding macrobiochar with a high-speed smashing machine and sieving the product using a stainless-steel mesh (pore size = 74 μm) [48]. The resulting biochar colloids were suspended in water, and the nanobiochar was separated from the supernatant and collected. Researchers have also used a disc mill, instead of a ball-mill, to break down biochar to a smaller scale. In one study, the ground biochar was suspended in ethanol, and after centrifugation, the suspension was dried and the nanofraction was collected [49]. A similar method was followed by Liu et al. (2018) in the preparation of goethite modified peanut shell biochar, wherein biochar powder was sifted out using a mesh of pore size 75–150 μm [18]. The colloidal biochar was suspended in water for 24 h to settle the particles larger than 100 nm. The remaining suspension was centrifuged, and the suspension, which contains nanobiochar, was pipetted out. Oleszczuk et al. (2016) and Lian et al. (2018) followed a similar strategy in the preparation of grass, wheat straw, and rice husk nanobiochar, with changes only in mesh size, which were 500 μm and 50 μm, respectively [29, 60].

A different process was used by Genovese et al. (2015) to prepare exfoliated biochar nanosheets using corn cob as the feedstock material [11]. Corn cob chunks were soaked in 1 M HNO_3 at 75 °C for 4 h as a pre-treatment before charring. After pyrolysis, the oxidized carbon was thermally exfoliated via flash heat treatment at 950 °C for 45 s, inside of a high-temperature muffle furnace, as a post-treatment [28]. This particular method helps to obtain nanosheets without subjecting the material to mechanical processes which may break down its particle size.

In a study by Wallace et al. (2019), softwood was subjected to microwave pyrolysis for 25–50 min at three different microwave power levels, 2100, 2400, and 2700 W [34]. This method may be more convenient because nanobiochar is directly produced without any further preparation process. A microwave absorber was used to increase the reaction temperature in a nitrogen atmosphere, wherein 1 kg of biomass was mixed with the microwave absorber (10 wt%) and pyrolyzed for a residence time of 60 min [73], [34].

Table 3. Fabrication techniques used for nanobiochar preparation other than ball-milling (NBC)

Nanobiochar type	Feedstock material	Temperature/ Power °C/W	BET surface area (m^2/g)	Preparation method	Sieve type	Other methods	Reference
Wood biochar	Pitch pine	600 °C	-	High-speed smashing machine	200-mesh stainless steel screen with a 74 µm mesh size	-	[48]
	Dendro	700–1000 °C	28	Disc mill	-	Biochar (BC) preconditioned at −80 °C for three days before being ground using disc mill. The BC was dispersed in ethanol, and the supernatant was collected and dried. The dried layer of NBC was scraped off.	[49]
Goethite modified peanut shell biochar (PSB)	Peanut shell	300 °C	63.6	-	Sifted with a mesh 75–150 µm	NBC suspension was carefully pipetted and collected from the supernatant of the centrifuged BC suspension	[18]
		400 °C	78.6				
		500 °C	230				
		600 °C	264				
Grass biochar	Elephant grass (BC-m) (*Miscanthus*)	700 °C	36.39	-	-	BC dispersion was sonicated and passed through a 500 µm sieve. The sieved suspension was centrifuged, and supernatant with NBC was separated.	[29]
	Wicker (BC-w)	700 °C	18.25				
Wheat straw biochar	Wheat straw (BC-	700 °C	29.56				

	s)						
Exfoliated biochar nanosheets	Corn cob	900 °C	543.7	-	-	Pre-treatment: Soaking in 1 M HNO_3 (20 ml) at 75 °C for 4 h; Post-treatment: HNO_3 oxidation and thermal flash. (45 s at 950 °C)	28
Rice straw biochar	Rice straw	400 °C	93.28	-	-	BC suspension was sonicated and passed through a 50 μm sieve and centrifuged. The supernatant was carefully collected and freeze-dried.	60
		700 °C	253.9				
		-	-	-	-	Powdered BC was separated by sieving and stirred with water. Supernatant was collected and dried at 60 °C for 5 h.	27
Rice hull biochae	Rice hull	300 °C	21.7	-	-	BC suspension was carefully pipetted after 2h and centrifuged. The obtained supernatant was collected and freeze-dried.	61
		400 °C	80.1				
		500 °C	90.9				
		600 °C	123.2				
Softwood biochar	Softwood chips	2100 W	14.44	Microwave pyrolysis	-	-	34
		2400 W	28.65				
		2700 W	9.96				
	Hemp stalk	2100 W	11.72				
		2400 W	12.26				
		2700 W	12.18				
Plant source biomass	Pinewood, wood chips, barley grass, wheat	500 °C	-	Slow pyrolysis	60-mesh sieve	Sieved biochar was dispersed in deionized (DI) water and stirred for 1 min, subjected to ultrasound for 30 min, and then stirred again for 10 min. The suspensions were allowed to settle for 24 h, and solid	47

	straw, peanut shell, rice husk					and liquid was separated via siphonage. Suspensions were further centrifuged at 3500 ×g for 30 min to obtain the supernatant containing the fractions of particle size <100 nm	
Municipal source biomass	Dairy manure, pig manure, sewage sludge						
Bagasse biochar	Bagasse	900 °C	620.87	Slow pyrolysis	-	Biochar was dissolved in ultrapure water and dispersed by ultrasonication for 10 min. The suspension was centrifuged at 5000 rpm for 3 min, and the supernatant were collected with a filter membrane (220 nm) and dried in an oven	36
Carbonaceous nanomaterials	Dairy manure	700 °C	-	Fluidized bed/pyrolysis	1 mm mesh	Biochar solutions were centrifuged at 5000 rpm for 20 min and the supernatant was separated. The supernatant was mixed with acetone, centrifuged at 5000 rpm for 20 min and supernatant was dried. Dried biochar was resuspended in water, and ultrasonicated for 1 min (200 W).	56
	Rice straw and sorghum straw	500 °C	-				

View Article Online
DOI: 10.1039/D0EN00486C

3.0 Properties of nanobiochar

The wide range of biochar characteristics allows for numerous applications in diverse fields. Successfully producing these properties depends on the feedstock material, and the process conditions utilized in the preparation process. Nanobiochar, which is prepared via reduction in the particle size of the same biochar, may demonstrate characteristics similar to those of macrobiochar; however, in many cases nanobiochar manifests characteristics considerably different from those at the macro scale, such as surface area.

3.1 Physical properties

3.1.1 Surface area

Biochar has a high surface area due to the large number of pores typically present in the material [74]. The amount of volatile gases released in the carbonization process directly influences the total surface area. However, hydrothermal carbonization reduces the surface area, whereas high surface area is a characteristic of biochar produced through pyrolysis [19]. Theoretically, nanoparticles should be characterized by reasonably high surface areas as compared to that of particles at the macro scale. Nevertheless, the literature has reported data that demonstrate comparatively high surface areas, typically measured using a BET analyzer, for some nanobiochar types at particular pyrolysis temperatures. However, significant differences in surface area have been exhibited at different pyrolysis temperatures. Therefore, no consistent correlation can be observed between the particle size and the surface area.

Nanobiochars produced at low temperatures, such as 300 and 400 °C, have low surface areas, from 5.6 to 47.2 m^2/g, respectively, whereas a significantly higher surface area range (342 to 430 m^2/g) results at high temperatures, such as 450 and 600 °C, respectively [38,39,57]. The increase in surface area is anticipated due to the devolatilization of biomass materials and development of pores on the surface of the material. Destruction of alkyl and ester functional groups during pyrolysis may account for high surface area [75]. However, surface area is governed by the hemicellulose content in the biomass. Even at high temperature conditions, nanobiochar produced from high lignin biomass demonstrates comparatively lower surface area than those produced from hemicellulose rich biomass [76]. Hence, modification methodologies have been used to increase the surface areas of lignin rich biochars [4,38].

Rice straw nanobiochar at 400 °C exhibited a noteworthy decrease in surface area, from 141.3 to 93.28 m^2/g, as compared to that of macrobiochar at the same temperature [60]. Conversely, at 700 °C, macrobiochar had less surface area than that of nanobiochar. When the temperature was increased to 700 °C, rice straw nanobiochar exhibited an increase in the surface area, as was expected. Furthermore, rice hull nanobiochar at 600 °C has exhibited a comparatively low surface area of 123 m^2/g, while macrobiochar at the same temperature results in a surface area of 27 m^2/g [61]. However, both rice husk and corn straw nanobiochars have high surface areas of 298 and 364 m^2/g at 500 °C, a relatively low pyrolysis temperature as compared to rice hull biochar [52]. However, the relative surface areas of macrobiochar and nanobiochar may depend on the nanobiochar preparation method as well. In the milling process, fine particles of biochar may clog the pores, leading to a decrease in the surface area. Nevertheless, research on tuning the surface area of nanobiochar is lacking, and more studies are recommended for a proper understanding.

At present, there is not sufficient information to conclude how surface area is increased or decreased with respect to feedstock at the same pyrolysis temperature. Iron oxide permeated mesoporous rice-husk nanobiochars prepared at 600 °C exhibited a high surface area, at 1736.8 m^2/g [4]. Pinewood nanobiochar prepared via pyrolysis at 525 °C possessed a surface area of 47.3 m^2/g [72]. Grass and wheat straw nanobiochar types, investigated by Nath et al. (2019), demonstrated a comparatively high surface area of 36.39 m^2/g for elephant grass (*Miscanthus*), whereas wicker and wheat straw nanobiochar had no significant difference in surface area compared to that of unmilled macrobiochar at 700 °C [29]. Magnetically modified ball-milled wheat straw nanobiochar had a greater increase in surface area, from 47.2 to 296.3 m^2/g, with increasing temperature, compared to that of pristine magnetic nanobiochar (from 2.93 to 198.6 m^2/g) [57]. Meanwhile, the considerably high surface area of 543.7 m^2/g exhibited by corn-cob-exfoliated biochar nanosheets is far higher than that of the macroscale corn cob biochar (7.9 m^2/g) [28]. It is important to note that the milling process may influence the internal and external surface areas. A recent study suggested that only the external surface areas increased during the ball-milling process probably without influencing the internal surface area [37]. Internal surface area governs the electron transfer ability, where high electron exchange ability improves the electrocatalytic activity.

Researchers have used various pre-conditioning methods prior to the milling process, which may induce the production of ultra-small particles [28,49]. The effect of pre-conditioning step and different milling conditions such as the ball material, amount and size, biochar : ball mass ratio

and solvent used may directly influence the particle size and surface area of the resulting nanobiochar.

3.1.2 Fixed carbon, volatile matter, and yield

Volatile matter is released from biomass at temperatures of around 950 °C [77]. Proximate analysis (wt%) of a softwood nanobiochar revealed a composition of 25% volatile matter and 71.3% fixed carbon (Table 4) [34]. However, the type of biomass directly influences the volatile matter percentage, and other softwood biomass such as cinnamon can release more volatile matter than that of general softwood biomasses. Interestingly, pinewood nanobiochar, which is prepared from resinous hardwood, has been reported to have a volatile matter content of 97% and a significantly low fixed carbon content of 1% [72]. Literature confirms that macro-scale softwood biochar, such as dendro biochar, exhibits a volatile matter content of 19.7% and fixed carbon content of 63.8%. According to the reported data, there is not a significant change in fixed carbon and volatile matter contents with respect to the particle size [78]. However, Oleszczuk et al. (2016) has reported that elemental content of macro and nanobiochar can vary considerably with particle size [79]. Furthermore, a positive trend was reported between the color and the yield of nano and microscale of biochars [47]. Both nano and micro fractions have demonstrated similar patterns. A suspension having a darker color gave higher yields, whereas lighter color gave lower yields. For, example, barley grass biochar with dark color suspensions (dark) yielded 20.5%, whereas pinewood biochar suspensions (light) yielded 1.43% [47].

3.1.3 Water-holding capacity

The pyrolysis process and the porosity of the parent material directly influence the hydrologic properties of biochar. With increasing pyrolysis temperatures, the number of surface functional groups is decreased, resulting in lower binding capacity to water and increased hydrophobicity [80,81]. The higher the number of functional groups, the higher the affinity towards water [19]. Therefore, based on the pyrolysis temperature, no significant difference in water-holding capacity is observed with respect to decreasing particle size. However, the ability to retain water within the material also depends on the porosity and coordination of the pores. Reportedly, pinewood nanobiochars prepared via pyrolysis at 525 and 400 °C have water holding capacities of 9.75 and 2.7, respectively [72, 82]. Nevertheless, owing to the limited number

of studies, the comparison of the limited data was too inadequate to be conclusive. Biochars with low production temperatures also contain pores, which are too small to hold a considerable amount of water because of poor interconnectedness and coagulation of the pores with remaining components, such as tar, depending on the feedstock [83].

3.1.4 Mechanical stability and grindability

Untreated biomass demonstrates anisotropic mechanical properties. However, the anisotropic effect becomes weak during the carbonization process, owing to the loss of structural complexity of the biochar. Therefore, biochar possesses poor mechanical stability compared to that of the parent biomass [84], [85]. Nevertheless, both macro and nano scales exhibit poor mechanical stability, which thus does not depend on the particle size.

Mechanical stability is inversely correlated with the porosity of the biochar [86]. Highly porous biochars have low strength, and processing methods like grinding create cracks in the structure, which result in the release of volatile matter and evaporation of water. Therefore, nanobiochar tends to be poor in strength [87]. However, establishing a better comparison of mechanical stability is, again, tricky because of the limited number of studies. Therefore, conclusions may not be valid for all biochar types. Production characteristics should be tested widely with varying conditions and a considerable number of samples. Given the correlation between mechanical stability and porosity, nanoscale particles will demonstrate high mechanical stability as compared to macrobiochars, owing to the low porosity in the particles.

Carbonization during torrefaction, which is known as mild-pyrolysis, adds brittleness to terrified biomass in the preparation process, which leads to improved grindability [19]. According to the Hardgrove grindability index (HGI), torrefied biomasses with high amounts of hemicellulose demonstrate better grindability [88]. Conducting fiber analysis of the biomass prior to torrefaction would provide information useful to choosing biomass with high amounts of hemicellulose [76]. Therefore, both preparation processes and feedstock materials govern the grindability of biochars. Torrefaction breaks down the physical or chemical structure of the internal tissues, for instance, cellulose, hemicellulose and lignin [89]. Literature reports that grindability has been evaluated by sample size distribution [76]. Chen et al. (2011) has reported 24,000 revolutions per minute (rpm) for 1 min as the proper conditions optimal grindability of bio-coal [76]. The energy required for grinding depends on the production temperature, and

View Article Online
DOI: 10.1039/D0EN00486C

different milling processes for particle size reduction can be compared based on this factor.[90] The energy demand for grindability is significantly reduced when dry, fresh biomass is used.

Table 4. Physicochemical properties of nanobiochar

	Properties											
Parent nanobiochar type	**EC**	**pH**	**Zeta potential (mV)**	**Specific gravity**	**Moisture content**	**Ash content**	**Volatile matter %**	**Fixed carbon %**	**C %**	**H %**	**N %**	**Reference**
Pinewood nanobiochar (525 °C)	1737	6.6	-31.3	0.4	2.11	2.0	97.0	1.06	83	3.5	<1	[72]
Elephant grass nanobiochar (700 °C)	-	7.8	-83.6	-	-	24.74	-	-	56.16	2.44	0.38	[29]
Wicker nanobiochar (700 °C)				-	-	30.97	-	-	51.57	2.11	0.44	[29]
Wheat straw nanobiochar (700 °C)	-	9.1	-88.4	-	-	52.35	-	-	27.88	1.55	0.11	[29]
Softwood nanobiochar (2700 W)	-	-	-	-	2.7	1.0	25.0	71.3	78.54	3.25	0.59	[34]
Dairy manure nanobiochar (500 °C)	-	9.76	-30.2	-	-	56.6	-	-	6.58	1.77	-	[47]

View Article Online
DOI: 10.1039/D0EN00486C

3.1.5 Zeta potential and colloidal stability

The zeta potentials of nanobiochars have been measured to understand their aggregation, electrokinetics, and stability [47,91]. A negative surface charge is prominent in both micro and nanobiochars because of the deprotonation of surface functional groups, which typically contain oxygen [92]. The zeta potential of biochars depends on the particle size and type of feedstock [47]. Therefore, nanobiochars demonstrate lower stabilities than those of corresponding micro or macrobiochars. This phenomenon has been observed in a zeta potential study done by Song et al. (2019), which revealed less negativity in the zeta potential values of micro and nanosuspensions of biochars (1.73–13.4 mV). Furthermore, the chemical composition of the feedstock, such as the contents of the carboxylic and phenolic groups, influences the zeta potential [93]. This inference was corroborated with data from Song et al. (2019), which revealed high zeta potentials for nanobiochars from plant sources than for nanobiochars from municipal sources. Hence, the nanobiochars that have less zeta potential and fewer O-containing functional groups resulted in more particles in suspension with limited settling. In addition, environmental factors, ionic strength, and pH of the media play a role in the stability and transportation of biochar. Nanobiochars manufactured from plants with different aggregation patterns (e.g., rich in lignin) and municipal waste have exhibited distinctly different effects in the presence of electrolytes. Nanobiochars rich in lignin showed no effect with changing electrolytes, whereas municipal waste nanobiochars with fewer phenolic and carboxylic groups exhibited high hydrodynamic particle diameters with the increase in electrolyte concentrations, which influences the electrostatic double layer [47]. No discrete difference in stability was observed based on the particle size; hence, the electrostatic repulsion alone cannot account for the stability of nanobiochars [94]. However, some research studies have confirmed that ball-milled biochars have exhibited greater stability and smaller particle size than unmilled biochars [37]. Chemical structures and compounds of the feedstock are proven the parameters that predominantly govern the stability of the resulting nanobiochars.

3.1.6 Agglomeration potential

Particles agglomerate in the form of pellets or granules with increased strength and density. Tumble agglomeration, which is also known as growth agglomeration, involves the growth of pellets or granules during a tumbling process, while press agglomeration involves the growth of agglomerates via the application of pressure [19].

The lignin content of the biomass plays a significant role in the pelleting process because of the high number of carboxylic and phenolic groups. During the process, lignin softens and acts as a natural binder. Therefore, woody biomass with high lignin contents result in more stable pellets compared to those obtained from low-lignin biomass [95]. According to literature, the moisture content of the biomass influences the softening point of lignin in the temperature range from 90 °C (wet-based) to 200 °C (dry-based) [96]. Other than the amount of lignin, rearrangement of particles and filling of intra-particle voids enhances the stability of pellets [19]. However, according to literature, agglomeration potential is subject to the composition of the biomass [47]. Further, nanobiochar particles may begin to agglomerate with the protonation of functional groups and concomitant reduction of surface charge in acidic environments [52].

3.1.7 Fluorescence activity

The fluorescence property has been observed and reported by carbon dots produced from different carbonaceous feedstocks and utilized for heavy metal sensing; however, studies on nanobiochars are lacking. A recent study focused their attention on three different nanobiochars, dairy manure, rice straw and sorghum straw biochar-derived carbonaceous nanomaterials as probes for sensing Hg, Pb, Ni and Cu through fluorescence quenching and fluorescence recovery [56]. It is suggested that the unshared electron pairs of the C—O, C=O and C—OH groups in carboxylic and phenolic functional groups in nanobiochars form coordination linkages with heavy metal ions [97]. Importantly, the same study indicated the cost effectiveness of the nanobiochars as electrode sensor materials indicating the price of nanobiochar as 18-times higher value than the pristine biochar (0.076 £/kg) and 1% of the market value of Carbon dots (129 £/kg). However, more studies that are detailed are needed in the field of fluorescence properties of nanobiochars and their use in sensor development since some of the metals showed less effectiveness.

3.2 Chemical properties

3.2.1 Elemental composition

The chemical composition of raw biomass is transformed primarily into carbon in the production of biochar. With decreasing particle size, from the macro scale to nanoscale, an apparent reduction in the carbon content has been observed. Wood chip biochars in macro, micro, and nano scales resulted in carbon contents of 81.2, 63, and 17.7%, respectively [47].

Owing to the disconnection of functional groups, oxygen and hydrogen contents are reduced, whereas the carbon content is correspondingly increased [19]. The carbon content is directly proportional to the pyrolysis temperature and carbon content of the feedstock material.

The H:C ratio of a biochar indicates its stability and aromaticity [98]. Softwood and hemp nanobiochars demonstrate higher carbon content (< 1.2) in the H:C ratio and also graphitic-like structures, which may increase the structural strength of a composite material (Table 4) [34]. Similarly, nanobiochar from pinewood, which is a hardwood, has been reported to have an H:C ratio of 0.5 [72]. Oleszczuk et al. (2016) reported elephant grass (*Miscanthus*), wicker and corn straw nanobiochars having an H:C ratio of 0.5, and wheat straw nanobiochar having an H:C ratio of 0.66 [29 52]. The least reported H:C ratio for nanobiochars has been recorded for rice husk nanobiochar, which is 0.17 [52]. However, macrobiochars of similar feedstock materials do not exhibit substantial differences in the H:C ratio as compared to that of nanoscale biochars. Although wheat straw biochar were prepared by Oleszczuk et al. (2016a) and Zhang et al. (2019) at a similar pyrolysis temperature, the H:C ratios were very different (0.66 and 0.02 respectively), which may be due to the inclusion of both nano and colloidal fractions in the resulting ball-milled biochar [53]. The high ratio of H:C in nanobiochar confirms considerable differences in its properties over ball-milled biochar that includes both colloidal and nano-sized fractions.

The polarity of a biochar is reflected by its O:C ratio. Wheat straw nanobiochar exhibits an O:C ratio of 0.48, whereas elephant grass and wicker nanobiochar produce similar values, at 0.21. A very recent study demonstrates an increasing pattern of both O:C and H:C ratios with respect to decreasing particle size [47]. Nano and microbiochars exhibit the lowest aromaticities, with higher H:C ratios compared to that of the macrobichars. On the other hand, there is not sufficient data to confirm a relationship between the nano and macro scales with regard to the O:C ratio. Micro and nanobiochars reportedly tend to have more aliphatic chains and functional groups at the macro scale [47]; however, this characteristic depends on the pyrolysis temperature and the feedstock material, owing to the loss of functional groups at high temperatures [49].

A study using Raman Spectroscopy and Electron-spin resonance studies provided a crucial understanding of the chemical changes taken during the milling process. The study indicated that the ROS pool noticeably reacts to form novel locally organized biochar structures showing a positive correlation with the milling time, and reaching chemical stability after the milling

process stops [99]. The generated ROS may be used for greener functionalization of nanobiochar catalysts before they reach stability.

3.2.2 Structural composition

Plant-based biomass is rich in cellulose, hemicellulose, and lignin, which helps in strengthening the structure. Most of the properties of biomass undergo remarkable changes as the pyrolysis temperature varies between 250 and 350 °C, owing to the complete and partial decompositions of hemicellulose, cellulose, and lignin. Wallace et al. (2019) reported the Fourier-transform infrared (FTIR) spectra of softwood nanobiochar, which confirms the presence of cellulose, hemicellulose, and lignin [34]. Despite the presence of these chemical compounds, the pore structures of softwood and hemp nanobiochar provide evidence, in microwave pyrolysis, of cracking with increasing power levels. The availability of residual tars inside the pores has been investigated, and a pattern of an increasing number of residual tars has been observed with respect to temperature [34].

The mineral composition of biochar is directly influenced by the feedstock sources. A dominant peak of SiO_2 was observed for plant biochars, such as wood and agricultural waste, whereas sludge-, municipal-, and animal-source biochars exhibit mineral peaks of $CaCO_3$, $Ca_3(PO_4)$, and aluminosilicate. Nano and micro biochars also presented sharp mineral peaks compared to those of macro biochars [47,49].

3.2.3 pH

Between the pyrolysis method and hydrothermal carbonization, the method of preparation causes significant changes in the pH of the resulting biochar [19]. Similarly, feedstock type also strongly impacts the alkalinity of the biochar, which can be acidified and its pH reduced via an acid-activation step [100]. Biochar is used as a soil amendment, and therefore the pH of biochar is important for agricultural applications. High-cellulose and lignin-containing biochars, such as pinewood nanobiochar, demonstrate slightly alkaline pH of 6.6 [72]. Nevertheless, elephant grass (*Miscanthus*), wicker, and wheat straw nanobiochars, with comparatively low amounts of cellulose and lignin, possess highly alkaline pH levels of 7.8, 8.9, and 9.1 respectively (Table 4) [29].

The alkalinity of biochar is influenced by four broad categories: soluble organic compounds, surface organic functional groups, carbonates, and other inorganic alkalis [101]. The amounts of organic compounds, such as cellulose and lignin, essential oils, and resins, can directly affect

the alkalinity of a biochar, depending on the feedstock material. Goethite-modified peanut shell nanobiochar exhibits similar pH (6.4 and 6.8) at the low temperatures of 300 and 400 °C, respectively. However, a slight increase in pH (7.08 and 7.28) can be observed at higher temperatures of 500 and 600 °C, respectively, owing to high ash content produced in the pyrolysis of biomass [3,18]. Among many types of biochars, those derived from wood exhibit high alkalinities (pH > 8). Pinewood (pH 6.3) and wood chip (pH 7.05) biochars demonstrate weakly acidic or neutral pH, which may be due to relatively low ash content and loss of carboxyl groups; however, the nano and micro fractions of wood-derived biochars have higher pH (pH 8.9–9.7) than those particles at the macro scale [102]. Agricultural waste and manure-derived biochars also possess high pH (pH 10.0–10.4). Nevertheless, the micro and nano fractions exhibit slightly lower pH values, up to 9.5, which may be due to the loss of inorganic substances, such as Ca, P, and S [103]. Sewage sludge biochar at the macro, nano, and micro scales do not show any differences in pH values [47].

3.2.4 Surface chemistry

Surface functional groups present in nanobiochar primarily vary with the feedstock material and the pyrolysis temperature. Owing to the increasing temperature, volatile organic compounds of the material can devolatilize, which leads to a reduction of surface functional groups. However, literature confirms that ball-milled biochar contains more oxygen containing functional groups (2.2-4.4 mmol/g) compared to unmilled pristine biochars (0.8-2.9 mmol/g) [37]. Additionally, the number of acidic surface functional groups increases after ball-milling, so that adsorption performance can be enhanced [35,59] . Further, milling exposes the graphitic nature of the nanobiochars and induces ROS formation, which may improve its surface chemistry than that of the pristine biochars. Most of the studies have used FTIR spectroscopy to identify surface functional groups and some have quantified those with Boehm titration [34,35]. In bagasse biochar, acidic functional groups concentrations were shown to increase from 0.8 to 2.5 mmol/g following by the milling process [35]. However, this increase may be due to solvents used for milling. By using various types of solvents, such as water and ethanol, the number of acidic surface functional groups (O—H) can be increased [49,104]. Aromatic C=C/C=O, O—H, COOH and C—H [41] are the most common surface functional groups observed on nanobiochars [4,35]. Apart from those, N—H bonds and SiO_2 are also present depending on the feedstock material [34]. A comparatively high number of functional groups (e.g., –COOH, –COOC) and newly evolving aliphatic chains have been determined to be present in nano and micro fractions of biochar, as compared to macrobiochar [105,106], evidenced by substantial increases in –OH

stretching (3400 cm^{-1}) and C–O stretching in nanobiochars samples [107]. The reduction of conjugated benzene rings is evidenced by the peak shifts of –C=C and –C=O, with decreasing particle size, and the nano and micro fractions of biochar demonstrate the lowest aromaticities.

Reactive oxygen, rich in nanobiochars based on the production through milling, plays a strong role in various applications. Milling process governs surface chemistry of nanobiochars. Wet milling increased the surface functional groups and ash content of the resulting nanobiochars, however demonstrated a significant decrease in C content [62]. Therefore, careful selection of the milling process is important based on the application of the nanobiochar.

3.3 Mechanical properties

3.3.1 Hardness and Young's modulus

The ductility of a material can be measured using Young's modulus, whereas its strength can be represented by its hardness properties. However, there are few studies on the mechanical properties of nanobiochar. Wallace et al. (2019) have reported on both hardness and Young's modulus and confirmed that nanoscale particle size enhances the mechanical properties of a biochar. Both softwood and hemp nanobiochars demonstrate substantial increments in hardness and Young's modulus values with respect to increasing microwave power levels, which is similar to those observed for pyrolysis temperatures >300 °C [34]. Increasing the fixed carbon content and decreasing the volatile matter content with respect to pyrolysis temperature directly influences the enhancement of mechanical properties. The elastic behaviors of softwood and hemp nanobiochar have also been studied using nanoindentation tests, and their flexural strength properties have been confirmed. Therefore, nanobiochar shows great promise as a filler material in biocomposites [34].

4.0 Applications of nanobiochar

Nanobiochar has been used in diverse applications: as a contaminant removal material, catalyst, biomolecule carrier, electrode material, sensing material, an alternative for carbon black, and battery industry material (Figure 3) [35,43,65,108]. Furthermore, nanobiochar can be used as a material to enhance the growth of plants such as wheat and rice [27]. The majority of research publications on nanobiochar focus on its use as an adsorbent material (Table 1). The ability of nanobiochars to remove different substances, including both organic and inorganic compounds,

potentially toxic elements, agrochemicals, and pharmaceuticals, has been examined [35]. However, other than ball-milling for nanobiochar as a direct final product (Table 2), rest of the other techniques have resulted in a considerably low yield of nanobiochar, which is one of the main shortages in commercializing the product. Furthermore, high dispersibility in water has a possibility to release any associated contaminants into natural waters [18]. Moreover, moving to industrial-scale from lab-scale may emerge a number of issues in the milling process. Therefore, commercialise nanobiochar has to be further studied carefully and should conduct a techo-economic analysis [109].

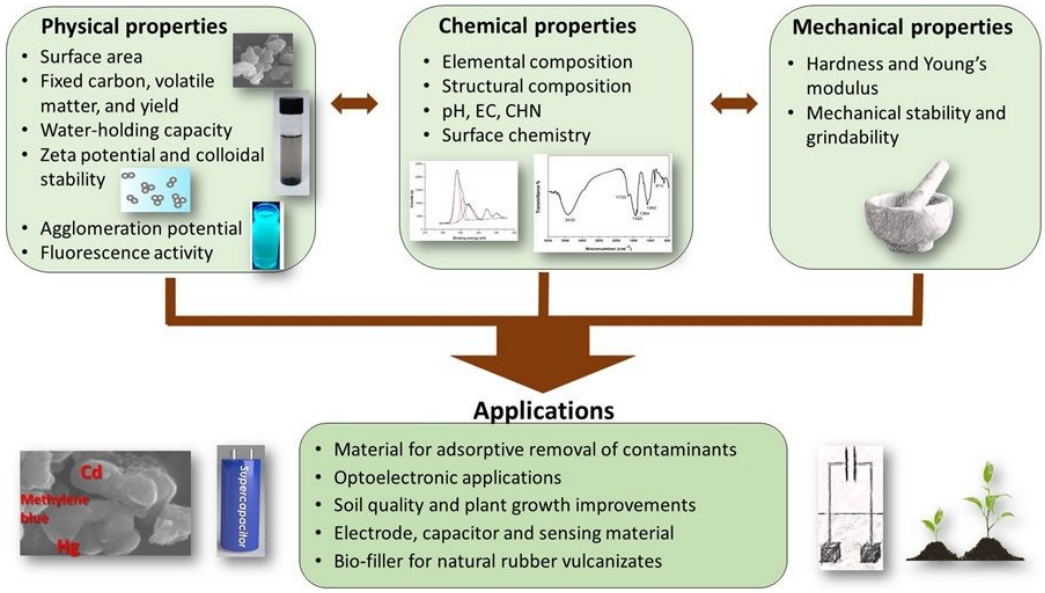

Figure 3. Applications of both pristine and modified nanobiochar (NBC) types

4.1 Materials for adsorptive removal of contaminants

Compared to carbonaceous materials, such as activated carbon, carbon nanotubes, and graphene oxides, pinewood nanobiochar exhibited higher adsorption capacities for organic substances, such as carbamazepine (95%) [45]. Adsorption potential of nanobiochars are based on variable charged functional groups, high surface area, graphitic nature and humic acid-like components. The capacity of woody nanobiochar for the removal of inorganic and organic micro-pollutants was examined by Ramanayaka et al. (2020), who demonstrated high removal capacities for 83, 520, 922 and, 7.46 mg/g for glyphosate, oxytetracycline, Cd(II) and Cr(VI), respectively due to the presence of different functional groups such as –OH, C==O, and –NH. However, physisorption was the primary removal mechanism, which indicates that nanobiochar may transport and desorb of such contaminants in water [49].

Nanobiochar is abundant in ROS, which may influence the degradation of organics such as glyphosate and oxytetracycline. However, research on the degradation of organic contaminants by the presence of ROS during the adsorption process is lacking [46]. Changing the physical, chemical, and mechanical properties of the biochar can also enhance its adsorption ability. Increasing solution pH from acidic to basic using a surfactant, such as Tween 80, can also boost the adsorption capacity of pinewood nanobiochar by 57% [72]. Goethite modified peanut shell nanobiochar formed intercalated heterostructures and induced heteroaggregation, which enhanced its adsorption performance [18]. Rice-straw-derived nanobiochar was mixed with goethite to form a composite that was then used to remove phenanthrene, demonstrating a maximum adsorption capacity of 253.9 mg/g at 700 °C [48]. Sugarcane bagasse nanobiochar delivered a methylene blue removal capacity 20 times higher than that of the pristine biochar due to increased external and internal surface areas and oxygen-containing functional groups which contributed to higher π–π and electrostatic attractions as compared to the pristine biochar [30]. However, no data are reported about the degradation of methylene blue by the presence of ROS from nanobiochar. In particular, nanobiochars that are rich in ROS may play an important role in organic contaminant degradation through photocatalytic actions. Harvesting ROS from nanobiochar before it becomes chemically stable remains an outstanding research challenge.

A recent study assessed the feasibility of wheat straw nanobiochar and its magnetized version on removing tetracycline and Hg(II) from water, indicating enhanced removal capacities. Increased removal of tetracycline was mainly governed by the combination of surface complexation and physisorption processes, i.e. electrostatic interactions, hydrogen bonds, and Cπ–Cπ interactions [57]. Nevertheless, a handful of literature reports adsorption performances of ball-milled biochar, inclusive of nano and colloidal fractions. These measured adsorption capacities are far less than that of the nanobiochar based on the calculated partitioning coefficients (PC) [38,51,63,66,110].

4.1.1 Adsorption performance of nanobiochar

Adsorption performances of materials can be compared using partitioning coefficients (PC). Using this approach, limitations that occur due to different initial concentrations and conditions are possible to overcome. The ratio between the maximum adsorption capacity (mg/g) and equilibrium concentration of adsorbate (mg/L) represents the PC value of a particular adsorbent [49,111].

In the adsorption of methylene blue, ball-milled sugarcane bagasse nanobiochar (BMBG450) having a pyrolysis temperature of 450 °C exhibited a comparatively high PC value of 3.6 L/g, while pristine sugarcane bagasse biochar (BG450) had a value of 0.1 L/g at pH of 4.5. However, with increasing pH of the media, PC values of both BG450 and BMBG450 decreased to 0.08 and 2.83 L/g respectively. Therefore, the best adsorption performance was exhibited by sugarcane bagasse nanobiochar over macrobiochar, which may be due to the high surface area (331 m^2/g) and methylene blue speciation [30]. Corn straw (CS) and rice husk (RH) nanobiochars demonstrated PC values of 0.03 and 0.02 L/g for phthalate esters and with increasing pH, PC values were slightly increased up to 0.08 and 0.06 L/g respectively [52]. At low pH, repulsive forces between nanobiochar particles decrease, leading to substantial agglomeration. In addition, low pH decreases pore-filling mechanisms and adsorption capacity [52]. Moreover, rice straw nanobiochar produced at pyrolysis temperatures of 400 and 700 °C demonstrates PC values of 2.12 and 4.4 L/g, respectively, for the adsorption of Phenanthrene (Figure 4). At 700 °C, rice straw nanobiochar (N700) has an almost two-fold increase in PC value versus 400 °C [60]. The high PC value of N700 may be due to its high specific surface area of 253.9 m^2/g. Bamboo biochar has been used in the adsorption of ammonium from water, and ball-milled bamboo biochar (450 °C) has demonstrated two times higher adsorption performance (0.1 L/g) over unmilled biochar (0.05 L/g) [41]. An interesting study reported enhanced sorption of CO_2 and reactive red using hickory wood (HC) and baggase N-doped and ball-milled biochar (BG) compared with pristine macrobiochar at two different temperatures (450 and 600 °C) [38]. N doped ball-milled biochars of both feedstock materials, regardless the temperature, demonstrated high PC values over pristine ball-milled biochar and macrobiochar (Figure 4).

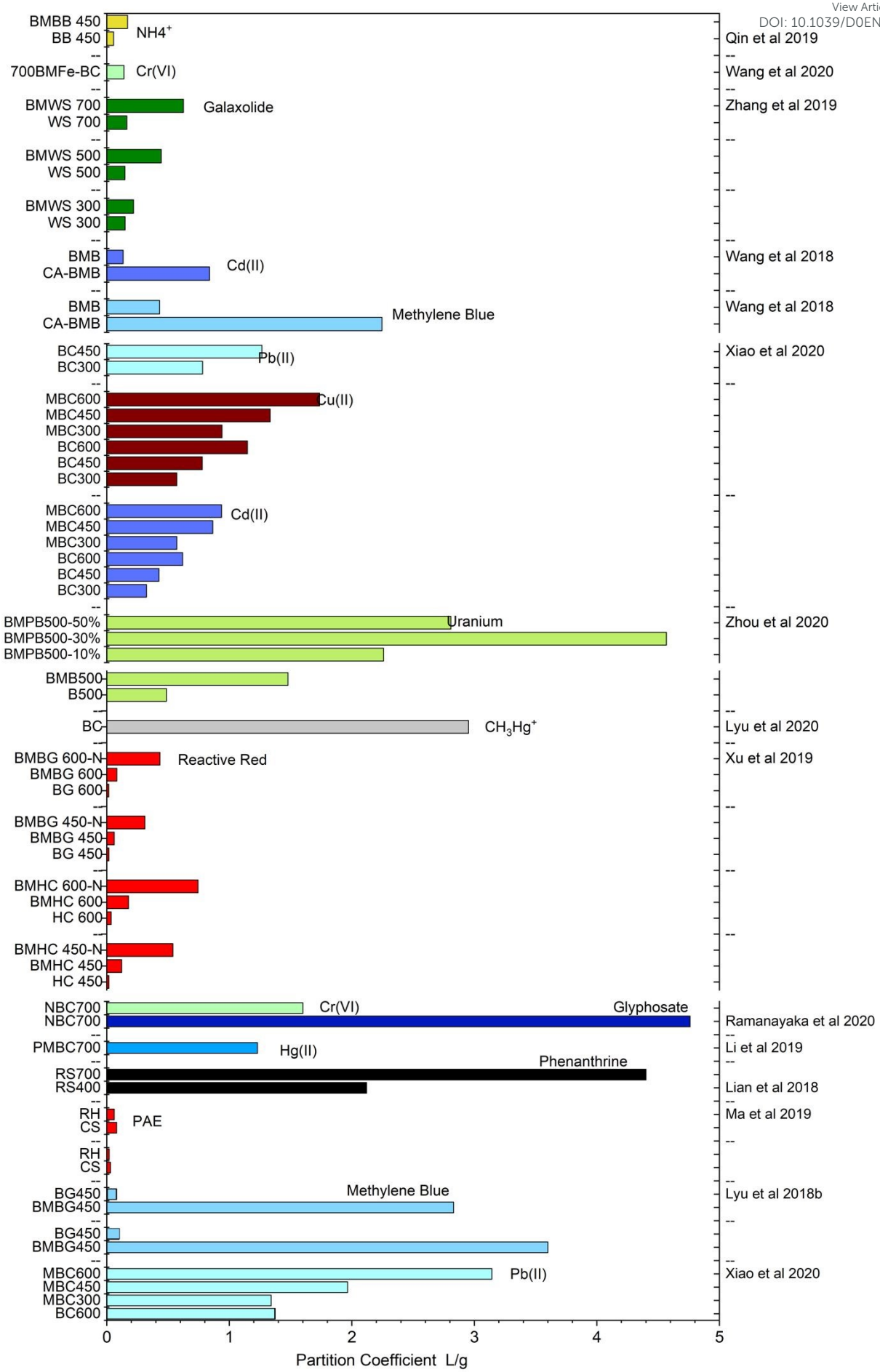

Figure 4. Partitioning coefficient (PC) values of nanobiochars to remove a variety of contaminants (Only partitioning coefficients less than 5 L/g were used to draw this graph). Note: BMBB: Ball-milled bamboo biochar, BB: Bamboo biochar, BMFe-BC: Ball-milled iron-biochar composite, BMWS: Ball-milled wheat straw biochar, WS: Wheat straw biochar, BMB: Ball-milled biochar, CA-BMB: Ball-milled bamboo biochar in Calcium-alginate beads, BC: born biochar, MBC: Ball-milled born biochar, BMPB: Ball-milled phytic acid biochar, BC: Thiol modified biochar, BMBG; Ball-milled bagasse biochar, BMBG-N: Nitrogen doped ball-milled bagasse biochar, BG: Bagasse biochar, BMHC: Ball-milled hickory chip biochar, BMHC-N: Nitrogen doped ball-milled hickory chip biochar, HC: Hickory chip biochar, NBC: Dendro nanobiochar, PMBC: Pristine magnetic biochar, RS: Rice straw biochar, RH: Rice husk biochar, CS: Corn straw biochar

4.2 Optoelectronic applications

Nanobiochar has shown photocatalytic activity, which can be useful in the degradation of pharmaceuticals in water. For an example, a high Enrofloxacin removal rate of 80.2% with a mineralization rate of 66.4% was achieved by nanobiochar via the involvement of $\bullet O_2-$ and *h*+ as dominant mechanisms during the photodegradation process [46].

Interestingly, literature revealed that nanobiochars disperse minerals, becoming efficient adsorbents and, at the same time, potential vectors for organic contaminants by forming stable clusters in their environments [18,60]. Nanobiochar is water-dispersible and hence can be used in versatile film-forming techniques for the preparation of film electrodes with potential applications in electrochemical fields. A few studies have been successful in using water-dispersible nanobiochar as an electrode material for Pb(II) and Cd(II) voltammetric sensors [48,112]. Furthermore, fluorescence analysis confirms that biochar releases dissolved organic matter (DOM) which contains humic-like fluorescent components [113]. These florescent properties of biochar nanomaterials have been used as fluorescence probes for heavy metal sensing specifically for Hg(II), Ni(II), Pb(II), and Cu(II) [56]. This was the very first study that reported utilizing quenching data of nanobiochar as an easy and accurate technique for toxic metal sensing. Moreover, functionalized magnetic baggase nanobiochar was prepared by incorporating carboxylic functional groups and enzymes for bisphenol A detection in water, showing both high sensitivity and outstanding electrochemical activity [36].

Aside from electrochemical sensors, the catalytic activity of nanobiochar has also been examined. Magnetic nanobiochar was sulfonated and assessed for its catalyst activity, showing

enhanced performance towards the esterification reaction [55]. In the battery industry, inexpensive, very-high-yield graphite should be used in anodes (Table 1), and so the substitution of graphite has been tested using nanobiochar produced via the modification of biochar to synthesize biochar graphite [108]. The graphitic nanobiochar is known as potato flakes by battery chemists. Recently, ball-milled nanobiochars have demonstrated prominent electrochemical properties as ideal carbon electrode materials for energy application, over the pristine biochars with poor catalytic performance and low electrical conductivity [114]. The latest research reports that high internal surface area, abundant pores, large amount of oxygen-containing functional groups, and graphitic structure, facilitates the electron transfer thereby reducing interface resistance [37]. Further, high temperature nanobiochars showed the best electrocatalytic activity with many hundred thousand times less cost as compared to Pt-electrodes, indicating its capacity for future research and development as an energy material.

4.3 Soil and plant improvements

Other than utilization as a material for adsorptive removal, optoelectronic applications and energy storage, additional applications for nanobiochar have been tested, including as solid fuel briquettes for pellet biofuels, and other purposes, such as rice bio-fertilizers [48]. Water-soluble carbon nanoparticles (wsCNPs) from acid modified nutrient loaded (e. g. NO_3^- and NH_4^+) rice husk biochar has confirmed the fast germination of wheat seeds [27]. An increasing growth rate of shoots has been observed with concentration ranges of wsCNPs from 10 – 50 mg/L over 5 days. Similar increases in shoot length have been observed within 20 days. Moreover, wsCNP concentrations above 50 mg/L, result in a slight decrease in growth rate compared to a loading of 50 mg/L. Therefore, high concentrations of wsCNPs may result in excess stress on the growth rate of shoots [27]. However, the data in this study show that nutrient concentrations have been increased during the course of this study, and thus insufficient information to conclude that decreased plant growth rate is related to biochar particle size. Moreover, Hernandez-Soriano et al. (2016) reported that biochar contains high DOM content which can positively impact plant growth [113]. During the milling process, DOM can be released in elevated concentrations, conditioning the soil for better plant growth.

Yue et al. (2018) studied the effect of nanobiochar on rice plant growth and the uptake of Cd^{2+}. High pyrolysis temperature nanobiochar (500 and 600 °C) resulted in a significant reduction of the uptake and phytotoxicity of Cd^{2+} compared to low-temperature (300 and 400 °C)

nanobiochar and macro biochar. A remarkable reduction of Cd^{2+} as toxicity, the stress on rice seedlings, and induced oxidative stress on rice plants was also demonstrated with high-temperature nanobiochars [61]. Nanobiochar has been applied as a material to protect native environments and plants by reducing the stress of invasive plants. Furthermore, nanobiochar has shown promise in enhancing rice seedlings and biomass, increasing the length of the root and chlorophyll concentrations, while reducing oxidative stress. However, the potential risks of applying nanobiochar should be further investigated [64]. Further, nanobiochar has its potential to be an effective plant nanobionics material as a functional nanomaterial to improve the plant productivity. In this case, nanobiochar will possibly be used as a nanocarrier for pesticides, nutrient/plant growth compounds to improve yield.

4.4 Other applications

Biochars are not that appropriate as electrode materials due to low specific capacitance, their powdered nature, and relatively low electrical conductivity. Nanobiochars that have been utilized for supercapacitors showed promising results; both top-bottom and bottom-up methods have been able to fabricate nanobiochars for strong supercapacitors [14,32,115]. Literature confirms that biomass-derived carbon nanofibers are capable of storing energy up to 791 F/g, which is higher than the capacity of three-dimensional (3D) structures [116]. The large specific surface area of nanobiochar facilitates the transport of charged ions during energy storage. Biomass with high cellulose fiber content contains nanofibers due to the presence of elemental fibril [117]. Moreover, owing to high ion storage capacity, interlayer distance, chemical stability and conductivity, carbonaceous materials like graphene and amorphous carbon have been utilized as supercapacitor electrode materials [117]. Acid pretreatment and polymer post treatments both reduced structural integrity and electrical conductivity [32]. Recently, an interesting study has been conducted to develop an alternative for carbon black, utilizing lignin-derived nanobiochar [65]. The resulting black liquor lignin nanobiochar has a graphitic and hydrophobic structure, which resulted in a high affinity toward rubber. Nanocomposites of styrene-butadiene rubber and lignin nanobiochar have led to improved vulcanization rates and tensile properties [65]. Another recent study reported the potential of ball-milled rice husk biochars as a novel bio-filler for natural rubber vulcanizates dsue to the synergistic effect of carbon and silica in pyrolized rice husk, resulting in better reinforcing performance than silica or biochar alone [54].

5.0 Techno-economic analysis

The capital cost, operating cost and estimated cost to prepare nanobiochar has been evaluated using previously conducted studies with respect to pyrolysis of hemicellulose rich biomass waste (e.g. corn cob), and using pre-treatment techniques to increase the brittleness [109]. Cost estimates done prior to scaled-up production will deliver an opportunity to choose the cheapest production method for a particular type of nanobiochar. However, it is necessary to consider the properties of the expected final product, which may affect the selected production method. The cost for equipment in preparation of nanobiochar is possible to obtain through a market survey or manufacturer questioning. The total plant cost (TPC) includes the total cost of base equipment, design, installation of plant, fabrication and modification of the system if needed. TPC comprises fixed capital investment (FCI), and start-up cost and working capital (15% of FCI) as well (Table S1) [118]. Based on the production methods, the FCI analysis demonstrates major cost variables; i.e., microwave pyrolysis results in a considerable increase in FCI due to high power consumption. Therefore, the total production cost for each process depends on the country and the production yield.

6.0 Risk and Toxicity of nanobiochar

The remarkable development of nanobiochar in the last few years has gained research attention owing to its growth potential in many applications. Therefore, the toxic effects of nanobiochar on plants and humans should be thoroughly investigated before large-scale industrial or agricultural applications are pursued (Figure 5). These effects can be varied in terms of either the physical or chemical effects of the biochar material [119].

Toxic effects relevant to plant systems can be varied in terms of cytotoxicity, genotoxicity, and ecotoxicity [120]. However, the toxic behavior of nanobiochar has not yet been thoroughly assessed. Therefore, thorough investigations of chemical reactions and pathways are needed to understand the toxic effects on both plant and mammalian cells. The influences of physicochemical properties on the toxicity also should be studied. Nanobiochar can sorb both organic and inorganic contaminants, and the ability to move with groundwater and surface water, making them a potential contaminant vector. Similarly, the presence of nanobiochar in water bodies may lead to toxic effects in both humans and animals due to ingestion and dermal contact. Further, the high activity of nanobiochar in alkaline conditions could create additional risks [52]. Due to the wide range of potential applications of nanobiochars, a study was conducted

to assess its toxicity on *Streptomyces*, a soil microorganism that produces two-thirds of the naturally-originating antibiotics. In this study, nanobiochar exhibited higher toxicity than carbon nanotubes and graphene [50]. It was further observed that the spherical shape of the nanobiochars, correlated for cell damage and high ROS, resulted in the strongest antibiotic production compared to other carbon nanomaterials, which may be a promising use of nanobiochar in the future. However, this recent study indicated the need of the ecotoxicity assessments before the large-scale use of nanobiochars in various applications.

The literature confirms that the ultra-small particle size, morphology, and hydrophobicity of nanobiochar can lead to interactions between these nanoparticles and cells that may cause damage to both plant and mammalian cells [121]. The toxicity of nanobiochar on plant systems is governed by the contribution of agglomeration, adsorption, and the reactivity of surface functional groups to the surrounding environment. Variations in toxicity levels depend on nanobiochar concentrations and degrees of agglomeration near plant roots. At low concentrations, no oxidative stress and no influence on the germination of seeds and on flowering have been observed [122].

Monocot plants positively respond to plant–nanobiochar interactions, whereas dicot plants exhibit both positive and negative responses [123]. The most common hypothesis on underivatized nanobiochar toxicity suggests that nanobiochars damage the soft membranes of cells. Nanobiochars, which can be dispersed in water, can be transported easily via the plant uptake through the xylem vessels [119].

Similar to plant cells, nanobiochar demonstrates toxic effects on mammalian cells. Trace metals and polycyclic aromatic hydrocarbons (PAHs) are present in biochars as primary toxicants [124]. Commonly used pyrolysis temperatures in the preparation of biochar are in the range of 400–500 °C, the particular temperature range in which most PAHs can be formed [125]. Both the trace metal content and concentration of PAHs depend on the feedstock material and the pyrolysis temperature. Trace metal concentrations further increases during pyrolysis [126]. Studies have proven that PAH exposure can cause broad-spectrum toxicity in human cells. Immobilized heavy metals in feedstock materials and contaminated feedstock materials also affects the resulting potential toxicity of biochars [127]. On the other hand, a review of recent literature confirms that no study has been conducted regarding the toxic effects of nanobiochars on mammalian cells [128].

View Article Online
DOI: 10.1039/D0EN00486C

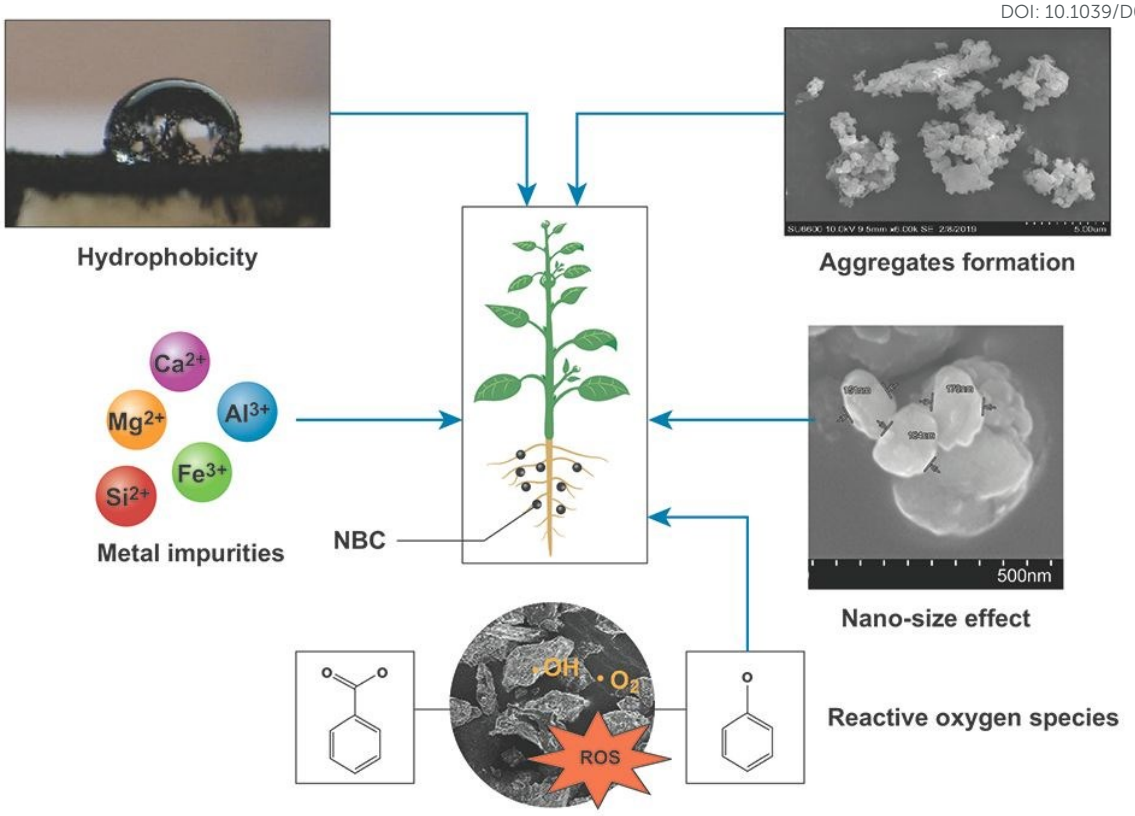

Figure 5. Factors responsible for the toxicity of nanobiochar in plant systems

However, toxicity on plant and mammalian systems has been interpreted as being mainly due to effects directly caused by the ultra-small particle size of the nanobiochar. The toxicity of PAHs on mammalian cell systems, on the other hand, has been investigated as the toxic effect directly caused by the presence of biochar. Literature to date suggests that the utilization of nanocarbons from biochar does not cause adverse effects to human health [27]. However, the toxic effects of nanobiochar on animals, humans and plants should be further investigated.

7.0 Future perspectives

The literature indicates expanding interest in the preparation of nanobiochar. Researchers have studied mechanical synthesis methods and direct methods of manufacturing nanobiochar. Moreover, research regarding the preparation and suitable applications of nanobiochar have increased in recent years.

Although many studies have been conducted on the synthesis of nanobiochar, we suggest further studies on milling processes to further elucidate potential relationships between the milling process and the properties of the resulting material. For, example, studying the preparation of nanobiochar using different grinding processes, such as ball-milling and dick milling, would be of value. Similarly, new approaches, such as microwave pyrolysis [129] , for the preparation of nanobiochar should be explored to introduce novel methods as an alternative to conventional methods such as milling. Correspondingly, direct nanobiochar preparation methods, such as the production of exfoliated nanobiochar from corn cob, should be further studied. Through the use of direct preparation methods, the morphology and topography of nanobiochar can be preserved and further studied.

Research work on proximate and ultimate analysis and the properties of nanobiochar require further study. More studies are needed to analyze the %C, %H, and %O, and other common properties, such as EC, zeta potential, and pH, to gain a clearer understanding of the characteristics of nanobiochar and how they vary with feedstock, pyrolysis conditions, and nanobiochar production technique. Similarly, the chemical, physical, and mechanical properties of biochar should be thoroughly investigated in order to identify relationships between the properties and type of nanobiochar.

Only a few studies have been conducted to assess the optoelectronic properties of nanobiochar. More attention is needed to develop nanobiochars as a high capacitance material in electronics industry and as a catalytic material in photocatalytic processes. Further, ROS reactions involving nanobiochar should be investigated, particularly their role in the degradation of organic substances in the environment. No such studies have been conducted to assess the degradation of organic compounds by reactive organic species of nanobiochar. At the same time, only a few studies have begun to demonstrate the potential of nanobiochar as a catalyst, functional material for semiconductors, as an energy storage and conversion material in capacitors and batteries. Ball-milled nano-activated carbon demonstrated 16 times higher specific capacitance more than that of the commercial ink, and 4 times higher than that of the original activated carbon, indicating the potential of nanobiochar in developing flexible coaxial fiber supercapacitors [115]. A recent research reports highlighted the capacity of ball-milled carbon nanomaterials, suggesting a promising future in energy conversion, energy storage and catalytic properties; however, the feedstocks were carbon nanotubes and graphene, not biochar, and hence more research in this field is encouraged [130]. Furthermore, it has been proven that higher hemicellulose amounts result in better grindability [76]. Therefore, properties of

nanobiochar derived from high hemicellulose content biomasses should be investigated in advance.

There are very few studies regarding the toxic effects of nanobiochar, and no studies have been conducted to investigate the toxicity of nanobiochar on mammalian cell systems. The effects of both nanoscale particle size and biochar material should be examined. The variability of PAHs profiles and concentrations with respect to the pyrolysis temperature and the feedstock material, and the amount of trace metals with respect to feedstock material all should be considered. Within plant systems, research can be conducted to study the effects of the shape of the nanobiochar particle within plant xylem systems.

Finally, studies that have already tested various possible applications of nanobiochar can be upgraded to include studies on its reusability. For example, research should be conducted to determine the regeneration ability of nanobiochar. Similarly, nanobiochar can be improved for applications in fields such as the removal of metal ions from water by upscaling to include nanobiochar in water filtration units. Additionally, low yields of nanobiochars during production is considered a bottleneck in the continued research into nanbiochar. Studies that focus on optimizing production, understanding chemical and physical properties, elucidating potential toxicity, and creating further value-added applications promise to move their utility and application forward. Further, nanobiochar has the potential to be developed as a tool for the slow releasing of nanofertilizer, nanocarrier plant nanobionics and in health care applications.

8.0 Conclusions

Nanobiochar has demonstrated excellent adsorption capacities for both toxic metals and organic contaminants, along with favorable catalytic and electrochemical properties. Moreover, nanobiochar has identified as a promising material in energy conversion and energy storage applications. However, as in the case of biochar, the properties depend upon the feedstock, preparation temperature, milling method, conditions and pretreatment. This review identified research gaps and challenges related to future development of nanobiochar research and their applications. The primary challenges are: (1) that most studies focus on ball-milled biochar, which include both colloidal and nano-sized fractions, and hence characterization is lacking for nanobiochar alone, (2) that there are limited large and field scale investigations due to low yields, creating a need for optimized preparation techniques for high yields, (3)

nanobiochar needs to be upscaled for energy and catalytic applications, (4) there is a lack of ecotoxicological information on the fate and transport of nanobiochar, (5) we lack a thorough understanding of chemical changes and changes in the transient ROS pool generated during milling, and (7) a cost-benefit analysis and life cycle assessment for various applications is much needed to move the application of nanobiochar forward.

Acknowledgement

This work was carried out with the support of "Cooperative Research Program for Agriculture Science and Technology Development (Project No. PJ01475801)", Rural Development Administration, Republic of Korea. This research was also supported by the Hydrogen Energy Innovation Technology Development Program of the National Research Foundation of Korea (NRF) funded by the Korean government (Ministry of Science and ICT (MSIT)) (No. NRF-2019M3E6A1064197).

References

1. Lehmann, J. Terra Preta Nova – Where to from Here? BT - Amazonian Dark Earths: Wim Sombroek's Vision. in (eds. Woods, W. I. et al.) 473–486 (Springer Netherlands, 2009). doi:10.1007/978-1-4020-9031-8_28
2. Manyà, J. J. Pyrolysis for biochar purposes: a review to establish current knowledge gaps and research needs. *Environ. Sci. Technol.* **46**, 7939–7954 (2012).
3. Ahmad, M. *et al.* Biochar as a sorbent for contaminant management in soil and water: a review. *Chemosphere* **99**, 19–33 (2014).
4. Nath, B. K., Chaliha, C. & Kalita, E. Iron oxide Permeated Mesoporous rice-husk nanobiochar (IPMN) mediated removal of dissolved arsenic (As): Chemometric modelling and adsorption dynamics. *J. Environ. Manage.* **246**, 397–409 (2019).
5. Libra, J. A. *et al.* Hydrothermal carbonization of biomass residuals: a comparative review of the chemistry, processes and applications of wet and dry pyrolysis. *Biofuels* **2**, 71–106 (2011).
6. Liu, W.-J., Jiang, H. & Yu, H.-Q. Development of biochar-based functional materials: toward a sustainable platform carbon material. *Chem. Rev.* **115**, 12251–12285 (2015).
7. Liu, W.-J., Li, W.-W., Jiang, H. & Yu, H.-Q. Fates of chemical elements in biomass during its pyrolysis. *Chem. Rev.* **117**, 6367–6398 (2017).
8. Liu, W.-J., Jiang, H. & Yu, H.-Q. Emerging applications of biochar-based materials for energy storage and conversion. *Energy Environ. Sci.* **12**, 1751–1779 (2019).
9. Strezov, V., Evans, T. J., Kan, T., Strezov, V. & Evans, T. J. Lignocellu-118. losic biomass pyrolysis: A review of product properties and effects o f pyrolysis parameters and effects of pyrolysis parameters. *Renewabl e Sustain. Energy Rev.* **57**, 1126–1140

(2015).
10. Li, X. T. *et al.* Biomass gasification in a circulating fluidized bed. *Biomass and bioenergy* **26**, 171–193 (2004).
11. Chen, W.-H., Peng, J. & Bi, X. T. A state-of-the-art review of biomass torrefaction, densification and applications. *Renew. Sustain. Energy Rev.* **44**, 847–866 (2015).
12. Huggins, T., Wang, H., Kearns, J., Jenkins, P. & Ren, Z. J. Biochar as a sustainable electrode material for electricity production in microbial fuel cells. *Bioresour. Technol.* **157**, 114–119 (2014).
13. de Oliveira, P. R. *et al.* The use of activated biochar for development of a sensitive electrochemical sensor for determination of methyl parathion. *J. Electroanal. Chem.* **799**, 602–608 (2017).
14. Genovese, M. & Lian, K. Polyoxometalate modified pine cone biochar carbon for supercapacitor electrodes. *J. Mater. Chem. A* **5**, 3939–3947 (2017).
15. Ok, Y. S., Chang, S. X., Gao, B. & Chung, H.-J. SMART biochar technology—A shifting paradigm towards advanced materials and healthcare research. *Environ. Technol. Innov.* **4**, 206–209 (2015).
16. Cao, X. & Harris, W. Properties of dairy-manure-derived biochar pertinent to its potential use in remediation. *Bioresour. Technol.* **101**, 5222–5228 (2010).
17. Zhang, X. *et al.* Using biochar for remediation of soils contaminated with heavy metals and organic pollutants. *Environ. Sci. Pollut. Res.* **20**, 8472–8483 (2013).
18. Liu, G. *et al.* Formation and physicochemical characteristics of nano biochar: insight into chemical and colloidal stability. *Environ. Sci. Technol.* **52**, 10369–10379 (2018).
19. Weber, K. & Quicker, P. Properties of biochar. *Fuel* **217**, 240–261 (2018).
20. Azargohar, R. & Dalai, A. K. Steam and KOH activation of biochar: Experimental and modeling studies. *Microporous Mesoporous Mater.* **110**, 413–421 (2008).
21. Kim, H.-B., Kim, J.-G., Kim, T., Alessi, D. S. & Baek, K. Mobility of arsenic in soil amended with biochar derived from biomass with different lignin contents: Relationships between lignin content and dissolved organic matter leaching. *Chem. Eng. J.* 124687 (2020).
22. Plötze, M. & Niemz, P. Porosity and pore size distribution of different wood types as determined by mercury intrusion porosimetry. *Eur. J. Wood Wood Prod.* **69**, 649–657 (2011).
23. Ohliger, A., Förster, M. & Kneer, R. Torrefaction of beechwood: A parametric study including heat of reaction and grindability. *Fuel* **104**, 607–613 (2013).
24. Naghdi, M. *et al.* A green method for production of nanobiochar by ball-milling-optimization and characterization. *J. Clean. Prod.* **164**, 1394–1405 (2017).
25. Xiao, D., Yuan, D., He, H. & Gao, M. Microwave assisted one-step green synthesis of fluorescent carbon nanoparticles from ionic liquids and their application as novel fluorescence probe for quercetin determination. *J. Lumin.* **140**, 120–125 (2013).
26. Liu, W.-J., Tian, K., Jiang, H. & Yu, H.-Q. Facile synthesis of highly efficient and recyclable magnetic solid acid from biomass waste. *Sci. Rep.* **3**, 2419 (2013).
27. Saxena, M., Maity, S. & Sarkar, S. Carbon nanoparticles in 'biochar'boost wheat (Triticum aestivum) plant growth. *Rsc Adv.* **4**, 39948–39954 (2014).
28. Genovese, M., Jiang, J., Lian, K. & Holm, N. High capacitive performance of exfoliated biochar nanosheets from biomass waste corn cob. *J. Mater. Chem. A* **3**, 2903–2913 (2015).
29. Oleszczuk, P., Ćwikła-Bundyra, W., Bogusz, A., Skwarek, E. & Ok, Y. S. Characterization of nanoparticles of biochars from different biomass. *J. Anal. Appl. Pyrolysis* **121**, 165–172 (2016).
30. Lyu, H. *et al.* Experimental and modeling investigations of ball-milled biochar for the

removal of aqueous methylene blue. *Chem. Eng. J.* **335**, 110–119 (2018).
31. Qin, Y. *et al.* Persistent free radicals in carbon-based materials on transformation of refractory organic contaminants (ROCs) in water: A critical review. *Water Res.* **137**, 130–143 (2018).
32. Li, X. *et al.* Flexible and Self-Healing Aqueous Supercapacitors for Low Temperature Applications: Polyampholyte Gel Electrolytes with Biochar Electrodes. *Sci. Rep.* **7**, 1685 (2017).
33. Luong, D. X. *et al.* Gram-scale bottom-up flash graphene synthesis. *Nature* 1–5 (2020).
34. Wallace, C. A., Afzal, M. T. & Saha, G. C. Effect of feedstock and microwave pyrolysis temperature on physio-chemical and nano-scale mechanical properties of biochar. *Bioresour. Bioprocess.* **6**, 33 (2019).
35. Lyu, H. *et al.* Effects of ball-milling on the physicochemical and sorptive properties of biochar: Experimental observations and governing mechanisms. *Environ. Pollut.* **233**, 54–63 (2018).
36. He, L. *et al.* Multi-layered enzyme coating on highly conductive magnetic biochar nanoparticles for bisphenol A sensing in water. *Chem. Eng. J.* **384**, 123276 (2020).
37. Lyu, H. *et al.* Ball-milled biochar for alternative carbon electrode. *Environ. Sci. Pollut. Res.* **26**, 14693–14702 (2019).
38. Xu, X., Zheng, Y., Gao, B. & Cao, X. N-doped biochar synthesized by a facile ball-milling method for enhanced sorption of CO2 and reactive red. *Chem. Eng. J.* **368**, 564–572 (2019).
39. Huang, J., Zimmerman, A. R., Chen, H. & Gao, B. Ball-milled biochar effectively removes sulfamethoxazole and sulfapyridine antibiotics from water and wastewater. *Environ. Pollut.* **258**, 113809 (2020).
40. Wang, B., Gao, B. & Wan, Y. Comparative study of calcium alginate, ball-milled biochar, and their composites on aqueous methylene blue adsorption. *Environ. Sci. Pollut. Res.* **26**, 11535–11541 (2019).
41. Qin, Y. *et al.* Enhanced removal of ammonium from water by ball-milled biochar. *Environ. Geochem. Health* 1–9 (2019).
42. Xiang, W. *et al.* Enhanced adsorption performance and governing mechanisms of ball-milled biochar for the removal of volatile organic compounds (VOCs). *Chem. Eng. J.* **385**, 123842 (2020).
43. Naghdi, M. *et al.* Fabrication of nanobiocatalyst using encapsulated laccase onto chitosan-nanobiochar composite. *Int. J. Biol. Macromol.* **124**, 530–536 (2019).
44. Naghdi, M. *et al.* Pinewood nanobiochar: A unique carrier for the immobilization of crude laccase by covalent bonding. *Int. J. Biol. Macromol.* **115**, 563–571 (2018).
45. Naghdi, M. *et al.* Pine-wood derived nanobiochar for removal of carbamazepine from aqueous media: Adsorption behavior and influential parameters. *Arab. J. Chem.* **12**, 5292–5301 (2019).
46. Xiao, Y., Lyu, H., Tang, J., Wang, K. & Sun, H. Effects of ball-milling on the photochemistry of biochar: Enrofloxacin degradation and possible mechanisms. *Chem. Eng. J.* **384**, 123311 (2020).
47. Song, B., Chen, M., Zhao, L., Qiu, H. & Cao, X. Physicochemical property and colloidal stability of micron- and nano-particle biochar derived from a variety of feedstock sources. *Sci. Total Environ.* **661**, 685–695 (2019).
48. Li, L. *et al.* Mass preparation of micro/nano-powders of biochar with water-dispersibility and their potential application. *New J. Chem.* **41**, 9649–9657 (2017).
49. Ramanayaka, S., Tsang, D. C. W., Hou, D., Ok, Y. S. & Vithanage, M. Green synthesis of graphitic nanobiochar for the removal of emerging contaminants in

aqueous media. *Sci. Total Environ.* **706**, (2020).
50. Liu, X., Tang, J., Wang, L., Liu, Q. & Liu, R. A comparative analysis of ball-milled biochar, graphene oxide, and multi-walled carbon nanotubes with respect to toxicity induction in Streptomyces. *J. Environ. Manage.* **243**, 308–317 (2019).
51. Lyu, H. *et al.* Thiol-modified biochar synthesized by a facile ball-milling method for enhanced sorption of inorganic Hg2+ and organic CH3Hg+. *J. Hazard. Mater.* **384**, 121357 (2020).
52. Ma, S., Jing, F., Sohi, S. P. & Chen, J. New insights into contrasting mechanisms for PAE adsorption on millimeter, micron-and nano-scale biochar. *Environ. Sci. Pollut. Res.* **26**, 18636–18650 (2019).
53. Zhang, Q. *et al.* Ball-milled biochar for galaxolide removal: Sorption performance and governing mechanisms. *Sci. Total Environ.* **659**, 1537–1545 (2019).
54. Xue, B. *et al.* A facile ball-milling method to produce sustainable pyrolytic rice husk bio-filler for reinforcement of rubber mechanical property. *Ind. Crops Prod.* **141**, 111791 (2019).
55. Jenie, S. N. A., Kristiani, A., Kustomo, Simanungkalit, S. & Mansur, D. Preparation of nanobiochar as magnetic solid acid catalyst by pyrolysis-carbonization from oil palm empty fruit bunches. in *AIP Conference Proceedings* **1904**, 20018 (AIP Publishing, 2017).
56. Plácido, J., Bustamante López, S., Meissner, K. E., Kelly, D. E. & Kelly, S. L. Multivariate analysis of biochar-derived carbonaceous nanomaterials for detection of heavy metal ions in aqueous systems. *Sci. Total Environ.* **688**, 751–761 (2019).
57. Li, R. *et al.* Removing tetracycline and Hg(II) with ball-milled magnetic nanobiochar and its potential on polluted irrigation water reclamation. *J. Hazard. Mater.* **384**, 121095 (2020).
58. Peterson, S. C., Jackson, M. A., Kim, S. & Palmquist, D. E. Increasing biochar surface area: Optimization of ball-milling parameters. *Powder Technol.* **228**, 115–120 (2012).
59. Wang, K., Sun, Y., Tang, J., He, J. & Sun, H. Aqueous Cr(VI) removal by a novel ball-milled Fe0-biochar composite: Role of biochar electron transfer capacity under high pyrolysis temperature. *Chemosphere* **241**, 125044 (2020).
60. Lian, F., Yu, W., Wang, Z. & Xing, B. New Insights into Black Carbon Nanoparticle-Induced Dispersibility of Goethite Colloids and Configuration-Dependent Sorption for Phenanthrene. *Environ. Sci. Technol.* **53**, 661–670 (2018).
61. Yue, L. *et al.* The effect of biochar nanoparticles on rice plant growth and the uptake of heavy metals: Implications for agronomic benefits and potential risk. *Sci. Total Environ.* **656**, 9–18 (2019).
62. Yuan, Y., Zhang, N. & Hu, X. Effects of wet and dry ball-milling on the physicochemical properties of sawdust derived-biochar. *Instrum. Sci. Technol.* 1–14 (2019).
63. Xiao, J., Hu, R. & Chen, G. Micro-nano-engineered nitrogenous bone biochar developed with a ball-milling technique for high-efficiency removal of aquatic Cd(II), Cu(II) and Pb(II). *J. Hazard. Mater.* **387**, 121980 (2020).
64. Shen, Y. *et al.* Role of nano-biochar in attenuating the allelopathic effect from Imperata cylindrica on rice seedlings. *Environ. Sci. Nano* **7**, 116–126 (2020).
65. Jiang, C. *et al.* Converting waste lignin into nano-biochar as a renewable substitute of carbon black for reinforcing styrene-butadiene rubber. *Waste Manag.* **102**, 732–742 (2020).
66. Zhou, Y. *et al.* Engineered phosphorous-functionalized biochar with enhanced porosity using phytic acid-assisted ball-milling for efficient and selective uptake of aquatic uranium. *J. Mol. Liq.* **303**, 112659 (2020).

67. Yusof, J. M., Salleh, M. A. M., Rashid, S. A., Ismail, I. & Adam, S. N. Characterisation of carbon particles (CPs) derived from dry milled kenaf biochar. *J. Eng. Sci. Technol.* 125–131 (2014).
68. Agar, D. & Wihersaari, M. Bio-coal, torrefied lignocellulosic resources – Key properties for its use in co-firing with fossil coal – Their status. *Biomass and Bioenergy* **44**, 107–111 (2012).
69. Charkhi, A., Kazemian, H. & Kazemeini, M. Optimized experimental design for natural clinoptilolite zeolite ball-milling to produce nano powders. *Powder Technol.* **203**, 389–396 (2010).
70. Shah, U. V *et al.* Effect of milling temperatures on surface area, surface energy and cohesion of pharmaceutical powders. *Int. J. Pharm.* **495**, 234–240 (2015).
71. Wang, B., Gao, B. & Wan, Y. Entrapment of ball-milled biochar in Ca-alginate beads for the removal of aqueous Cd(II). *J. Ind. Eng. Chem.* **61**, 161–168 (2018).
72. Naghdi, M. *et al.* Pine-wood derived nanobiochar for removal of carbamazepine from aqueous media: Adsorption behavior and influential parameters. *Arab. J. Chem.* (2016). doi:10.1016/j.arabjc.2016.12.025
73. Mokhtar, N. M., Ethaib, S. & Omar, R. EFFECTS OF MICROWAVE ABSORBERS ON THE PRODUCTS OF MICROWAVE PYROLYSIS OF OILY SLUDGE. *J. Eng. Sci. Technol.* **13**, 3313–3330 (2018).
74. Brewer, C. E. *et al.* New approaches to measuring biochar density and porosity. *Biomass and Bioenergy* **66**, 176–185 (2014).
75. Tomczyk, A., Sokołowska, Z. & Boguta, P. Biochar physicochemical properties: pyrolysis temperature and feedstock kind effects. *Rev. Environ. Sci. Bio/Technology* **19**, 191–215 (2020).
76. Chen, W.-H., Hsu, H.-C., Lu, K.-M., Lee, W.-J. & Lin, T.-C. Thermal pretreatment of wood (Lauan) block by torrefaction and its influence on the properties of the biomass. *Energy* **36**, 3012–3021 (2011).
77. Basu, P. Chapter 7-gasification theory. *Biomass Gasification, Pyrolysis Torrefaction (Second Ed. Acad. Press. Bost.* 199–248 (2013).
78. Mayakaduwa, S. S. *et al.* Equilibrium and kinetic mechanisms of woody biochar on aqueous glyphosate removal. *Chemosphere* **144**, 2516–2521 (2016).
79. Oleszczuk, P., Ćwikła-Bundyra, W., Bogusz, A., Skwarek, E. & Ok, Y. S. Characterization of nanoparticles of biochars from different biomass. *J. Anal. Appl. Pyrolysis* **121**, 165–172 (2016).
80. Alam, M. S. *et al.* Thermodynamic analysis of nickel (II) and zinc (II) adsorption to biochar. *Environ. Sci. Technol.* **52**, 6246–6255 (2018).
81. Alam, M. S. *et al.* Mechanisms of the removal of U (VI) from aqueous solution using biochar: a combined spectroscopic and modeling approach. *Environ. Sci. Technol.* **52**, 13057–13067 (2018).
82. Yu, O.-Y., Raichle, B. & Sink, S. Impact of biochar on the water holding capacity of loamy sand soil. *Int. J. Energy Environ. Eng.* **4**, 44 (2013).
83. Das, O. & Sarmah, A. K. The love–hate relationship of pyrolysis biochar and water: a perspective. *Sci. Total Environ.* **512**, 682–685 (2015).
84. Byrne, C. E. & Nagle, D. C. Carbonization of wood for advanced materials applications. *Carbon N. Y.* **35**, 259–266 (1997).
85. Iizuka, H., Fushitani, M., Okabe, T. & Saito, K. Mechanical properties of woodceramics: a porous carbon material. *J. Porous Mater.* **6**, 175–184 (1999).
86. Kumar, M., Verma, B. B. & Gupta, R. C. Mechanical properties of acacia and eucalyptus wood chars. *Energy sources* **21**, 675–685 (1999).
87. Noumi, E. S., Blin, J. & Rousset, P. Optimization of quality of charcoal for

steelmaking using statistical analysis approach. in (2014).
88. Phanphanich, M. & Mani, S. Impact of torrefaction on the grindability and fuel characteristics of forest biomass. *Bioresour. Technol.* **102**, 1246–1253 (2011).
89. Zhang, J. & Zhang, X. 15 - The thermochemical conversion of biomass into biofuels. in *Woodhead Publishing Series in Composites Science and Engineering* (eds. Verma, D., Fortunati, E., Jain, S. & Zhang Biopolymer-Based Materials, and Bioenergy, X. B. T.-B.) 327–368 (Woodhead Publishing, 2019). doi:https://doi.org/10.1016/B978-0-08-102426-3.00015-1
90. Bridgeman, T. G., Jones, J. M., Williams, A. & Waldron, D. J. An investigation of the grindability of two torrefied energy crops. *Fuel* **89**, 3911–3918 (2010).
91. Safari, S. *et al.* Biochar colloids and their use in contaminants removal. *Biochar* **1**, 151–162 (2019).
92. Yi, P., Pignatello, J. J., Uchimiya, M. & White, J. C. Heteroaggregation of cerium oxide nanoparticles and nanoparticles of pyrolyzed biomass. *Environ. Sci. Technol.* **49**, 13294–13303 (2015).
93. Qian, L. *et al.* Effective removal of heavy metal by biochar colloids under different pyrolysis temperatures. *Bioresour. Technol.* **206**, 217–224 (2016).
94. Xu, F. *et al.* Aggregation behavior of dissolved black carbon: implications for vertical mass flux and fractionation in aquatic systems. *Environ. Sci. Technol.* **51**, 13723–13732 (2017).
95. Föhr, J., Ranta, T., Suikki, J. & Soininen, H. Manufacturing of torrefied pellets without a binder from different raw wood materials in the pilot plant. *Wood Res* **62**, 481–494 (2017).
96. Thek, G. & Obernberger, I. The pellet handbook: the production and thermal utilization of biomass pellets. (2012).
97. Plácido, J., Bustamante-López, S., Meissner, K. E., Kelly, D. E. & Kelly, S. L. Microalgae biochar-derived carbon dots and their application in heavy metal sensing in aqueous systems. *Sci. Total Environ.* **656**, 531–539 (2019).
98. Zhang, M. & Ok, Y. S. Biochar soil amendment for sustainable agriculture with carbon and contaminant sequestration. *Carbon Manag.* **5**, 255–257 (2014).
99. Heckley, E. M., Toto, J. J. & Venegas, J. M. Structural Changes of Hydrothermally Treated Biochar with Ball-Milling. (2014).
100. Vithanage, M. *et al.* Acid-activated biochar increased sulfamethazine retention in soils. *Environ. Sci. Pollut. Res.* **22**, 2175–2186 (2015).
101. Cheah, S., Malone, S. C. & Feik, C. J. Speciation of sulfur in biochar produced from pyrolysis and gasification of oak and corn stover. *Environ. Sci. Technol.* **48**, 8474–8480 (2014).
102. Fidel, R. B., Laird, D. A., Thompson, M. L. & Lawrinenko, M. Characterization and quantification of biochar alkalinity. *Chemosphere* **167**, 367–373 (2017).
103. Zhao, Y., Feng, D., Zhang, Y., Huang, Y. & Sun, S. Effect of pyrolysis temperature on char structure and chemical speciation of alkali and alkaline earth metallic species in biochar. *Fuel Process. Technol.* **141**, 54–60 (2016).
104. Munkhbayar, B. *et al.* Influence of dry and wet ball-milling on dispersion characteristics of the multi-walled carbon nanotubes in aqueous solution with and without surfactant. *Powder Technol.* **234**, 132–140 (2013).
105. Qu, X. *et al.* Chemical and structural properties of dissolved black carbon released from biochars. *Carbon N. Y.* **96**, 759–767 (2016).
106. Zhao, L., Cao, X., Mašek, O. & Zimmerman, A. Heterogeneity of biochar properties as a function of feedstock sources and production temperatures. *J. Hazard. Mater.* **256**, 1–9 (2013).

107. Keiluweit, M., Nico, P. S., Johnson, M. G. & Kleber, M. Dynamic molecular structure of plant biomass-derived black carbon (biochar). *Environ. Sci. Technol.* **44**, 1247–1253 (2010).
108. Banek, N. A., Abele, D. T., McKenzie Jr, K. R. & Wagner, M. J. Sustainable Conversion of Lignocellulose to High-Purity, Highly Crystalline Flake Potato Graphite. *ACS Sustain. Chem. Eng.* **6**, 13199–13207 (2018).
109. Lam, S. S. *et al.* Microwave vacuum pyrolysis of waste plastic and used cooking oil for simultaneous waste reduction and sustainable energy conversion: Recovery of cleaner liquid fuel and techno-economic analysis. *Renew. Sustain. Energy Rev.* **115**, 109359 (2019).
110. Zheng, Y., Wan, Y., Chen, J., Chen, H. & Gao, B. MgO modified biochar produced through ball-milling: A dual-functional adsorbent for removal of different contaminants. *Chemosphere* **243**, 125344 (2020).
111. Vikrant, K. & Kim, K.-H. Nanomaterials for the adsorptive treatment of Hg (II) ions from water. *Chem. Eng. J.* **358**, 264–282 (2019).
112. Liu, G. *et al.* Facile preparation of water-processable biochar based on pitch pine and its electrochemical application for cadmium ion sensing. *Int J Electrochem Sci* **11**, 1041–1054 (2016).
113. Hernandez-Soriano, M. C., Kerré, B., Kopittke, P. M., Horemans, B. & Smolders, E. Biochar affects carbon composition and stability in soil: a combined spectroscopy-microscopy study. *Sci. Rep.* **6**, 25127 (2016).
114. Cheng, B.-H., Zeng, R. J. & Jiang, H. Recent developments of post-modification of biochar for electrochemical energy storage. *Bioresour. Technol.* **246**, 224–233 (2017).
115. Zhang, R., Xu, Y., Harrison, D., Fyson, J. & Yang, Y. High-performance fibre supercapacitors based on ball-milled activated carbon nanoparticles mixed with pen ink. *J. Mater. Sci. Mater. Electron.* **30**, 20881–20891 (2019).
116. Azwar, E. *et al.* Transformation of biomass into carbon nanofiber for supercapacitor application – A review. *Int. J. Hydrogen Energy* **43**, 20811–20821 (2018).
117. Yang, C. *et al.* Flexible highly specific capacitance aerogel electrodes based on cellulose nanofibers, carbon nanotubes and polyaniline. *Electrochim. Acta* **182**, 264–271 (2015).
118. Islam, M. N. & Ani, F. N. Techno-economics of rice husk pyrolysis, conversion with catalytic treatment to produce liquid fuel. *Bioresour. Technol.* **73**, 67–75 (2000).
119. Bhati, A., Tripathi, K. M., Singh, A., Sarkar, S. & Sonkar, S. K. Exploration of nano carbons in relevance to plant systems. *New J. Chem.* **42**, 16411–16427 (2018).
120. Cifuentes, Z. *et al.* Absorption and translocation to the aerial part of magnetic carbon-coated nanoparticles through the root of different crop plants. *J. Nanobiotechnology* **8**, 26 (2010).
121. Chen, R. *et al.* Differential uptake of carbon nanoparticles by plant and mammalian cells. *Small* **6**, 612–617 (2010).
122. Dubey, P. *et al.* A simple one-step hydrothermal route towards water solubilization of carbon quantum dots from soya-nuggets for imaging applications. *RSC Adv.* **5**, 87528–87534 (2015).
123. Sonkar, S. K., Roy, M., Babar, D. G. & Sarkar, S. Water soluble carbon nano-onions from wood wool as growth promoters for gram plants. *Nanoscale* **4**, 7670–7675 (2012).
124. Freddo, A., Cai, C. & Reid, B. J. Environmental contextualisation of potential toxic elements and polycyclic aromatic hydrocarbons in biochar. *Environ. Pollut.* **171**, 18–24 (2012).
125. Oleszczuk, P. & Kołtowski, M. Changes of total and freely dissolved polycyclic

aromatic hydrocarbons and toxicity of biochars treated with various aging processes. *Environ. Pollut.* **237**, 65–73 (2018).

126. von Gunten, K. *et al.* Modified sequential extraction for biochar and petroleum coke: Metal release potential and its environmental implications. *Bioresour. Technol.* **236**, 106–110 (2017).
127. Ndirangu, S. M., Liu, Y., Xu, K. & Song, S. Risk Evaluation of Pyrolyzed Biochar from Multiple Wastes. *J. Chem.* **2019**, 4506314 (2019).
128. Dong, C. D. *et al.* Assessment of the pulmonary toxic potential of nano-tobacco stem-pyrolyzed biochars. *Environ. Sci. Nano* **6**, 1527–1535 (2019).
129. Yek, P. N. Y. *et al.* Microwave steam activation, an innovative pyrolysis approach to convert waste palm shell into highly microporous activated carbon. *J. Environ. Manage.* **236**, 245–253 (2019).
130. Lyu, H. *et al.* Ball-milled carbon nanomaterials for energy and environmental applications. *ACS Sustain. Chem. Eng.* **5**, 9568–9585 (2017).

View Article Online
DOI: 10.1039/D0EN00486C

Biochar conversion into nanobiochar induced multiple potential applications as an adsorbent, sensor, capacitor, photocatalytic and plant nanobionic material